5-2021

Automated Quality Control in Manufacturing Production Lines: A Robust Technique to Perform Product Quality Inspection

Mark Anthony Reyna
The University of Texas Rio Grande Valley

AUTOMATED QUALITY CONTROL IN MANUFACTURING PRODUCTION LINES: A ROBUST TECHNIQUE TO PERFORM PRODUCT QUALITY INSPECTION

A Thesis

by

MARK ANTHONY REYNA

Submitted to the Graduate College of
The University of Texas Rio Grande Valley
In partial fulfillment of the requirements for the degree of

MASTER OF ENGINEERING

May 2021

Major Subject: Electrical Engineering

AUTOMATED QUALITY CONTROL IN MANUFACTURING PRODUCTION LINES: A ROBUST TECHNIQUE TO PERFORM PRODUCT QUALITY INSPECTION

A Thesis
by
MARK REYNA

COMMITTEE MEMBERS

Dr. Satya Aditya Akundi
Co-Chair of Committee

Dr. Jia Chen
Co-Chair of Committee

Dr. Mostafizur Rahman
Committee Member

Dr. Yong Zhou
Committee Member

May 2021

ABSTRACT

Reyna, Mark A., Automated Quality Control in Manufacturing Production Lines: A Robust Technique to Perform Product Quality Inspection. Master of Science in Engineering (MSE), May, 2021, 84 pp., 15 tables, 28 figures, references, 45 titles.

Quality control (QC) in manufacturing processes is critical to ensuring consumers receive products with proper functionality and reliability. Faulty products can lead to additional costs for the manufacturer and damage trust in a brand. A growing trend in QC is the use of machine vision (MV) systems because of their noncontact inspection, high repeatability, and efficiency. This thesis presents a robust MV system developed to perform comparative dimensional inspection on diversely shaped samples. Perimeter, area, rectangularity, and circularity are determined in the dimensional inspection algorithm for a base item and test items. A score determined with the four obtained parameter values provides the likeness between the base item and a test item. Additionally, a surface defect inspection is offered capable of identifying scratches, dents, and markings. The dimensional and surface inspections are used in a QC industrial case study. The case study examines the existing QC system for an electric motor manufacturer and proposes the developed QC system to increase product inspection count and efficiency while maintaining accuracy and reliability. Finally, the QC system is integrated in a simulated product inspection line consisting of a robotic arm and conveyor belts. The simulated product inspection line could identify the correct defect in all tested items and demonstrated the system's automation capabilities.

DEDICATION

I am so grateful for the family and friends that supported me in completing this thesis and my graduate degree in electrical engineering. The care, motivation, and assistance my mother, Mary Reyna, and father, Tony Reyna, gave made it possible to chase my passion in engineering. My sister, Tanya Reyna, and brother, Daniel Reyna, helped me stay relaxed and smiling through the hardest times of 2020. My incredible cousins and friends were always there to talk, laugh, and dream with. To all these people in my life, thank you and I love you all. I look forward to what the future holds with you all in it.

ACKNOWLEDGMENTS

I am thankful to Dr. Satya Aditya Akundi, my thesis advisor, for all the resources and advice he shared. By allowing me to work at the Complex Engineering Systems Laboratory, pushing me to take on challenges I considered beyond my ability, and always being patient and welcoming with me, Dr. Akundi made it possible to complete this thesis and grow as an engineer. Thank you to my thesis committee members: Dr. Jia Chen, Dr. Mostafizur Rahman, and Dr. Yong Zhou.

I greatly appreciate Regal Beloit for providing a tour of their McAllen, Texas facility, demonstrating their equipment and processes, and providing samples and information on the discs built there.

TABLE OF CONTENTS

Page

LIST OF TABLES

Page

LIST OF FIGURES

Page

CHAPTER I

INTRODUCTION

In manufacturing, product quality refers to how a set of measured features of a product compare to a desired set of features. Some common quality features are dimensions, surface texture, coloration, ultimate strength, and mass. A few examples of product quality deviation are screws produced too thin, metal surfaces over-grinded, and poor automobile paintjobs. The difficulty in maintaining quality in manufacturing rises as product designs increase in complexity and an increase in yield. Part of the reason for this comes from an increased probability of machining errors, as well as possibly insufficient resources for quality inspection. For manufacturers to fulfill growing market demands and achieve acceptable quality levels, improvements in quality control (QC) are needed.

Quality control is defined by the American Society of Quality as “a part of quality management focused on fulfilling quality requirements” [1]. In other words, QC is the effort to maintain a level of quality across the production or use of an item. The standard to which a product is compared generally comes from a similar product, that is deemed to be ideal or in a satisfactory state. If a product’s quality attributes deviate from the standard, then it could result in being aesthetically unpleasing, having a reduced period of product usability, and/or failure to function properly, such as in the examples of quality deviations provided earlier. In the case of

just an aesthetic quality deviation, such as coloring or surface finish [2], the product may not appeal to potential customers leading to reduced sales or additional costs to improve appearance. Whereas in the case of functional failure, such as in automobile brakes, drastic consequences could result involving the loss or harm of human lives and expensive recalls. Therefore, QC is critical to any manufacturing process.

Since the start of mass production, the techniques used for QC have always depended on humans to some degree. Early QC techniques used human vision inspection as well as basic measuring tools handled by humans. Advancements to these early techniques led to improvements in existing tools accuracy and efficiency, examining new features, and developing methods for automating these measurements. Technological advancements then allowed for accurate and precise sensors to be integrated in factories for measurements, which automated tasks performed by quality inspectors. These sensors provide rich data with which can be analyzed for deeper insight on the performance of systems and tasks. Data analysis generally involves the use of machine learning (ML). The use of ML is ushering advanced manufacturing inspection techniques, and in remarkably automated and efficient ways. Lastly, an up-and-coming QC technique is machine vision (MV), which will directly challenge human vision inspection. Seeing the world, or production line, through camera lenses and programming systems to act appropriately on what is in view is the aim of MV.

Machine vision (MV) makes use of computer vision (CV), which has grown popular in recent years due to its increased use in notable applications such as self-driving vehicles [11], security systems [12], and drones [13]. MV uses CV to emulate the human vision system to gain information to be acted on. MV uses image processing techniques to identify or measure items in images to then be acted on. A MV system is comprised of at least a camera and a processor for

image processing and analysis. Some MV systems will include light sources, turntables, and robots to improve the inspection accuracy or viewing area. The potential of MV being used in QC systems has induced a wealth of research into the types of product defects detectable. Many MV systems are using QC features mentioned earlier, such as dimensions, color, and texture, to analyze products. The significance of MV as a form of QC inspection is their ability to perform repetitive tasks accurately and consistently for extended periods of time. Unlike humans, a QC system using MV will not tire out, can work at an efficiency unparalleled, and make fewer errors. Additionally, the efficiency at which MV performs is greatly enhancing the scale of products to be inspected. The success MV has had is increasing the scope, accuracy, and repeatability of QC for Industry 4.0 [15].

Although QC systems appears to be promising for the future, the current state of this technology is not universally on par with what is needed for absolute reliance on it. Progress continues to be made on sometimes low or volatile accuracy and precision. Researchers have made headway by developing novel algorithms or advancing existing algorithms to be more robust. Particularly, researchers are working on improving how these systems handle uncontrollable environmental conditions. Issues on lighting, background, and positioning of products for QC systems are largely considered in recent literature [16]. Additionally, the limits of current technology restrict the work developed, as accuracy suffers to reduce processing time [17]. Improvements in technology could result in shortened processing times and gained accuracy in the systems. Finally, fully automated QC systems are limited [18]. The need for some human intervention or validation in these systems is yet to be overcome.

This thesis presents a QC system developed to contribute to the body of knowledge addressing shortcoming of the technology. The proposed QC system can perform dimensional

and surface analysis in a production line; two common analyses MV systems are used for. Three notable features of the QC system are its ability to operate at high levels of automation, inspect complex shapes and figures, and adapt its inspection capabilities to new product types. To perform automated product inspection, the proposed QC system can make use of a robotic arm and conveyor belt which will allow for a stream of inspectable products to pass within its view. Once a decision on product quality has been made, the robotic arm can sort acceptable and defective items. More information on the system's automation capabilities is provided in Chapter 4, and experimental trials with a robotic arm and conveyor belt are demonstrated in Chapter 6. By using blob analysis, the QC system can trace complex shapes for data such as perimeter and area. The data collected is passed to an algorithm developed to assess the likeness between a base and test product. More information on this is shared in Chapter 4. Finally, the QC system is lightweight and can perform inspections by simply using a base item or manually inputted values. The QC system can perform accurate inspections at the millimeter scale making it suitable for use in many industrial applications. Chapter 6 provides a case study using the QC system on industrial metal discs used within electric motors.

The remainder of this thesis is structured as follows. Chapter 2 presents a literature survey on state-of-the-art QC systems developed for free-form analysis, dimensional analysis, and surface analysis. Chapter 3 introduces in detail the setup for the proposed QC system. Chapters 4 and 5 examine how the QC system performs dimensional and surface analysis, respectively. Chapter 6 provides an industry case study on the QC system for disc in electric motors. Additionally, the QC system is integrated in a simulated production line to demonstrate its automation capabilities. Chapter 7 concludes the research by discussing the abilities of the proposed QC system and future work.

CHAPTER II

LITERATURE SURVEY

The following is a literature survey covering state-of-the-art QC systems using MV for free-form analysis, dimensional analysis, and surface analysis for QC (a MV system in this chapter will refer to a QC system using MV). The research presented covers a wide range of applications in sectors such as manufacturing, agriculture, and construction.*

2.1- State of Research on Free-Form Product Inspection

Advancements in research on MV systems is leading to the prevalence of free-form object detection. Free-form objects have challenged researchers to address the need of advanced mathematical and statistical tools to be applied for inspection of complex shapes for products in manufacturing. Further, MV systems capable of performing free-form object detection are best suited to adapt to the continuously changing demands in manufacturing.

MV systems are capable of accurately detecting differences between 2D objects. Provided a baseline object and other objects to test against, MV systems can identify discrepancies between objects. This is an advantageous to manufacturers producing flat objects who can use this technology to rapidly identify defects and have them removed. An example of this technology was developed by Pacella *et al.* [19], who use a MV system to compare the profile of test objects with the profile of a baseline model. The difference in area between the

baseline and test objects is calculated and reported. The researchers of this system developed two approaches for determining the discrepancies: a single-segment approach and a multiple-segment approach. The single-segment approach uses a univariate synthetic measure and a univariate control chart for product differences. The multiple-segment approach uses a vector of discrepancy and multivariate control chart to measure and monitor product differences. Additionally, the two approaches can be used to identify shifting, scaling, and bending deformations and the extent of these deformations. The researchers demonstrated that the multiple-segment approach outperformed the single-segment approach in a case study on cut leather hides, due to its level of sensitivity.

It is essential that production tools be maintained to ensure output is at a desirable quality. In computer numerical controlled (CNC) machines that perform subtractive manufacturing by milling, the tools used for cutting and drilling degrade over time. MV systems offer a high-speed method for tool inspection allowing alerts to be made when tool replacement is necessary. Dai and Zhu [3] produced an automated MV system capable of inspecting micro CNC machine tools with the tool remaining in the machine, which further reduces machine downtime. It uses an algorithm that searches for bright pixels on the tool (indicative of wearing) then converts from pixels to millimeters (1.38 mm/pixel) to output the worn area. Figure 1 shows five images from the MV system of a progressively damaged tool at different time points. The researchers tested how their system performed under 12 varying CNC machine settings, such as varied spindle speed and radial engagement. The systems results found that a high level of precision can be achieved and how varying system's settings can extend a tool's life. Similarly, Chethan *et al.* [20] designed a MV system to observe and quantify the tool wear area on Nimonic 75-- a nickel-base super alloy. An acoustic emission (AE) sensor is used in addition to the MV

system for QC. The goal of the work is to optimize machining parameters using feedback from the MV signals and the AE sensor, along with the Taguchi technique, to reduce a tool's wear area. The MV system uses blob analysis outputting the wear area in pixels. An experiment conducted by the researchers found that optimizing the parameters using the two sensors in the QC system reduced the wear area by nearly 8.5%. Using the results, the researchers could precisely identify how changes in parameters, such as the tool's RPM and cutting depth, would affect wear area.

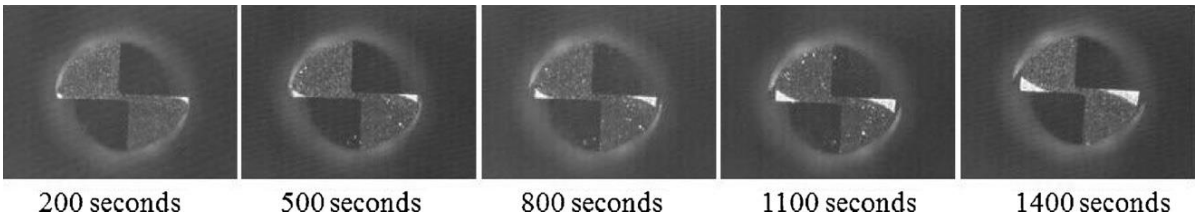

Figure 1: Growing Wear of Micro Tool (Source: Dai and Zhu [3])

Recycling is laborious process that is generally backed up. A major bottleneck in the process is accurately sorting the material inflow to avoid contamination later in the process. MV systems are used to some degree in many large recycling centers to improve the sorting efficiency. Research related to using MV systems for recycling aims to improve the accuracy which material is sorted, the range of material types, and innovative ways to make MV systems less expensive and more accessible. Wang *et al.* [21] propose a MV systems capable of sorting non-ferrous metals from end-of-life vehicles (ELV). The system can be used to categorize metal scraps of varying forms as either aluminum or copper. Four shapes are considered in the analysis of aluminum: rod, square, triangle, and round. Once some initial separating occurs, color and texture features are extracted from the materials. These features are used with principal component analysis (PCA) and support vector machine (SVM) to classify the metals at an

accuracy of 96.64%. Additionally, the system parameters were optimized for sorting the metal scraps at a sufficient accuracy and classification rate. The researchers performed an actual production test using their system and 170 kg of non-ferrous metal. The results of the case study showed the system could sort materials at an accuracy above 88.8% and a separation purity of 89.85%.

MV systems are growing in popularity for agricultural produce quality inspection. The tedious inspection process farmers and producers must undergo each season is shifting to MV systems, that can perform consistent and accurate inspections for longer periods of time. Su *et al.* [22] provide research on 3D quality inspection of produce, specifically potatoes, using MV systems. Performing inspections in 3D has allowed MV systems to determine potato volume and better identify appearance defects when compared to 2D. In this study, the system calculates the length, width, depth, fit ellipse, and surface area for each potato using three images. Using the acquired dimensional information, a linear regression model was created for predicting the mass of a potato. Once mass is estimated, the produce is classified into three categories: small, medium, and large. After sorting, the same images are passed through a series of detection algorithms for identifying: bumps, hollow areas, and/or bends in the potatoes. The MV system reached a 90% accuracy level for mass prediction and an 88% accuracy for defect categorization. Additionally, the work developed allowed for a virtual 3D reconstruction of the potatoes considered. This allows for the use of virtual reality (VR) as a method of remote quality inspection by humans. The MV system demonstrates how QC on agricultural produce can be performed in 3D and how mass, an unmeasurable property with cameras, can be reliably predicted using it.

Continuing on the agricultural applications of MV systems, Williams *et al.* [23] designed and tested a robotic kiwi harvesting system for commercial application due to the decreased a labor force in New Zealand. The system consists of five subsystems: MV for object detection, stereo depth location, a dynamic harvesting scheduler, arm path-planning and servo control, and fruit grip-and-depth. The first two subsystems mentioned are considered here. Successfully harvesting kiwis requires accurately detecting them. To find kiwis in an image, the researchers use a Fully-Convolution Network (FNC) for semantic segmentation. The FNC uses 48 images for training and 15 for validation. Once kiwis are identified in an image, the researchers used stereo image analysis to determine if the fruits are in a reachable range of the robotic arms, an example of this is shown in Figure 2. Fruits capable of being picked by the robotics arms are ordered by lowest hanging. Experimental results from the vision system show that 89.6% of pickable kiwis were correctly identified and that 76.0% of all fruit in the cameras field of view were detected. A cycle time of 5.5 s/fruit was reported, and a majority of that was attributed to the vision system.

Figure 2: MV System for Kiwi Identification (Source: Williams et al. [23])

Aquaculture, the cultivation of fish under controlled conditions, can improve tracking fish appetite which requires manual labor and involves subjectivity. Zhou et al. [24] offer a solution that uses a MV system to observe the fish feeding intensity, as shown in Figure 3. The system uses a near-infrared light source and camera for image acquisition. The researchers performed a rotation, scale, and translation technique on the fish feeding images, as well as a noise-invariant data expansion. The fish appetites were judged using a Convolution Neural Network trained on 8,800 images. The CNN achieved an accuracy of 90% and classified the feeding intensity better for "none" and "strong." A CNN was proven to outperform other classification methods in accuracy, such as support vector machine (73.75%) and back propagation neural network (81.25%). Additionally, CNN was preferred due to feature extraction occurring directly in the methods and better generality.

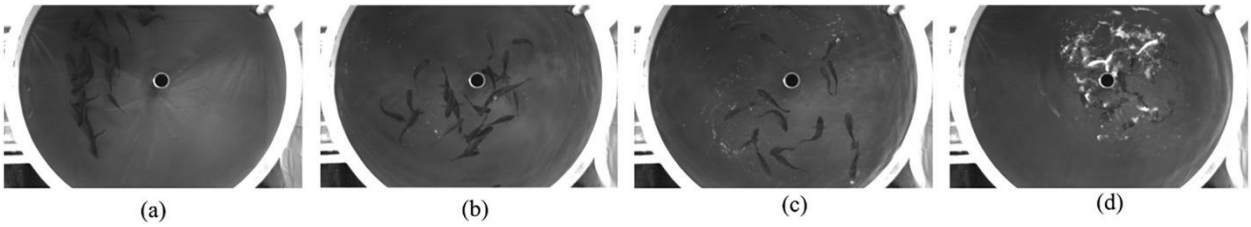

Figure 3: Fish Feeding Intensity (Source: Zhou et al. [25])

Similarly, harvesting fish is developing into an optimized and efficient, automated process. A MV system developed by Azarmdel *et al.* [25] is capable of gutting and cutting trout fish. The MV system developed determines the optimal cutting points for head removal and gut extraction. The series of procedures done to accomplish this does not rely on common machine learning methods, instead all image processing relied on tracing, coloring, and patterns on the fish. Essential to accurately determining the desired points of a fish was finding the four fins on its lower half. To do this the researchers first had to define a line through the upper and lower

half of a fish to divide the back and belly. A second line was then created on the lower half that allowed for easier identification of the fins using coloring techniques. Successfully segmenting the four fins required various combinations of cropping and thresholding through the entire procedure. The results of the system showed that fin identification could achieve a sensitivity, specificity, and accuracy of 86.054%, 99.965%, 99.874%, respectively. Accurately locating the fins provides improved head and belly mapping when compared to just determining the length and width of any fish, therefore optimizing the trout processing system.

Identifying fatigue crack initiation sites (FCIS) on metallic compounds is a task typically reserved for experts. However, Wang *et al.* [26] have created an automated system using MV for inspection of FCIS. To accomplish this Deeply Supervised Object Detector (DSOD) was created using Single Shot MultiBox Detector (SSD) combined with the DenseNet algorithm. Unfortunately, largely due to no datasets and minimal images on FCIS publicly available, the performance of the developed system could not reach a state in which the researchers believe it is ready to be used for practical applications. The results obtained showed that 38.5% of the bounding boxes outputted were totally invalid, yet 26.7% could excellently find an FCIS in an image. Nevertheless, the work contributed begins the investigation on how to automatically target FCIS.

Advancements in QC for e-jet printing systems were made by Lies *et al.*[27] who created a microlevel MV system. The system proposed performs in-situ inspection and is designed to be a step in a full closed-loop control system. Developing a system for small scale inspection required considerable effort to acquire high resolution images, and factors such as how the angular field of view was affected by the working distance were necessary to calculate. After image acquisition, all images were converted to greyscale and then binarized. Blob analysis was

used to obtain a scale of micrometers to pixels based on the known nozzle size. Using a created region of interest (ROI) on the images, morphological operations could be performed that improved determining the filament diameter. Finally, a 3D rendering was developed to imitate printed patterns and for analysis. The proposed system succeeded at detecting dimensional changes and handling multilayer inspection at the microlevel. The researchers identify the future direction of continuing to shrink the scale of the system to nanometer inspection.

A growing trend in home construction is pre-fabricating large home sections. The efficiencies of mass production allow for prefabricated sections to be quickly and cheaply produced. Martinez *et al.* [28] designed a MV system for manufacturing prefabricated home sections to ensure quality is maintained in the production of steel frames. Inspection is done on the studs of steel frames for mistakes such as improper squaring or positioning. A variety of steel frames appear in the construction process considered so the researchers developed a robust system capable of handling a range of frame complexities. To ensure correct frames were being produced, the model analyzed by the MV system was compared to the frame assembly model with an allowed tolerance. The system follows four modules: frame inspection algorithm, functional features extraction, inputs validation, and decision-making module (DMM). The frame inspection algorithm uses an adapted Hough transform for line detection, intersection detection, and stud detection. In the inputs validation module, studs detected are matched to the Building Information Module (BIM) and labelled. The DMM outputted either a warning that misplacements occurred but were within the tolerance or an error that misplacements occurred and need relocation or replacement. In three case-studies, one real and two virtual, the proposed system correctly performed stud detection and operation points estimation. Finally, the system

proposed is reported to delay the manufacturing process by 1.5-2% but could avoid greater delays of 35-55% caused by errors.

In summary, the identified case studies demonstrate the ability of MV systems to analyze products of complex forms and provide objective analyses on them. MV systems capable of free-form analysis expand the design options available to manufacturers by providing a platform and advances to efficiently inspect complex products and their geometries. Additionally, products that are by nature free-form and have been time consuming to inspect can be rapidly inspected through these MV systems.

2.2- State of Research on Product Dimensional Analysis

One of the most common uses for MV systems is in gaining dimensional information on a considered product. In QC, it's important to ensure that a product stays within a size tolerance. To verify production specifications are being satisfied, manufacturers are placing greater confidence in MV systems to perform accurate and efficient dimensional measurements. Recent literature on dimensional analysis for MV systems is demonstrating the range and complexity of problems being solved with it. Progress on program efficiency, scale of inspection, and environmental factors are just some of the issue's researchers are providing creative solutions for.

Gears are a commonly manufactured item that could benefit from increased accuracy and precision in inspection. Moru and Borro [29] improved QC for gear inspection by developing a MV system that assesses whether a produced gear exceeds a specified size tolerance, and then has a robot to automatically act on a decision made by the system. Using a telecentric camera

lens and high-performance equipment, subpixel level measurements of the gears were captured. Specifically, the outer diameter, inner diameter, and number of teeth were computed using a unique algorithm for each measurement. The determined measurements were then provided to an application developed by the researchers for comparison with an acceptable gear. Experimentation of the system was conducted on 12 gears with the system correctly rejecting 4 gears that did not meet the 0.02mm threshold specified. The system developed also considers measurement uncertainty when classifying and works with a significantly lower tolerance due to potential system errors.

As previously mentioned, a popular industrial application for MV systems is inspecting quality and safety of food. Devi *et al.* [30] contrived a MV system for inspection of rice grain sizes and quality. The system uses Canny Edge Detection to obtain the contour of each rice grain in an image, and then develops a region of interest (ROI) around the grain for classification. From the ROI, various properties such as length and breadth can be determined for each grain. In the results of an experiment, the system achieved over 90% classification accuracy. A deeper investigation on QC for rice grains was conducted by Chen *et al.* [31] The researchers considered only red indica rice, and developed a system that identified kernels that were broken, chalky, and damaged or spotted. Image acquisition was performed using a charge-coupled device (CCD) and a near infrared backlight. Each of the three types of defects previously mentioned required a unique algorithm. The broken kernels identification algorithm classified using a support vector machine (SVM) based on the length of each kernel. The chalky algorithm used the varying infrared light penetration through the kernels with another SVM to identify the chalky areas. The damaged and spotted areas algorithm performed edge detection using the Sobel gradient operator and Otsu segmentation to remove kernel contours. This allowed for inner defects to show and be

reported. Ultimately, the proposed system achieved accuracies of 99.3%, 96.3%, and 93.6% for the broken, chalky, and damaged or spotted algorithms, respectively. Additionally, the system had an average run time of 0.15 seconds making it efficient for colored rice inspection.

For carrot grading, Xie *et al.* [32] use a MV system to investigate 12 attributes of carrots—six on dimensions and six on color. The attributes determined are used as inputs in three ML algorithms which are compared for accuracy and speed in grading carrots. To determine the shape features, the system first performs pre-processing on the acquired images. Area, perimeter, and aspect ratio can be solved for prior to developing a tight ROI around the carrot to identify the length and maximum diameter. A carrot's average diameter is calculated by averaging the distance every 50 pixels of the carrot. Accuracy differences for back propagation neural network (BPNN), support vector machine (SVM), and extreme learning machine (ELM) were 93.33%, 91.67%, and 96.67%, respectively. In addition to reaching the greatest accuracy, ELM was praised for its processing time and generalization abilities.

Devi et al. [30], Chen et al. [31], and Xie et al. [32] demonstrate the progress being made in QC with application toward accurate dimensional detection of small objects with a potential application and reliance in manufacturing processes such as sorting, machining and quality management.

Improvements in the accuracy of glass bottle breakage and contamination detection were made by Huang *et al.* [33] The improvements come without sacrificing the number of bottles inspected. The MV system used for the inspection process involves multiple observation points which check the bottles mouth, bottom, and walls. Tracking a bottle's mouth is performed by using a radial scanning method followed by contour fitting. Next, feature extraction is done and,

finally, defect recognition capable of identifying multiple defects and providing dimensional information on the defect(s). To track a bottle's bottom, edge detection and bottom positioning are used. Fourier transform and inverse transform are used for texture smoothing of the images, and a blob algorithm is used to detect the specific defects on the bottom of the bottle. Examples of bottom defects capable of being detected are hairs and blunt areas. The MV system developed is also able to inspect the walls of an entire bottle for abnormal qualities and stains. Notably, the system maintains an inspection rate of 72,000 bottles per hour while achieving a defect detection rate of 100% and qualified bottle detection rate of 99.84%.

Large-scale additive manufacturing (LSAM) is a developing technology in construction that will allow for buildings and structures to be printed with building material (i.e., cement). Kazemian et al. [34] proposed a MV system for real-time quality control in construction involving LSAM. QC for this technology is limited yet essential for human safety, therefore the proposed inspection system attempts to fill the void by integrating MV to LSAM devices for layer-by-layer inspection. Attachment of the system to existing robotic devices was shown to be unobtrusive. The inspection system performs preprocessing to the extent that the images of the layer being extruded are isolated and converted to a binary image. The width of the layer determines whether the material is being over or under-extruded. Using a calibrated pixel per inch ratio, a conversion is easily available. The system performance showed inspection abilities down to an inch, and, as shown in Figure 4, was able to classify over and under-extruded layers. An early test of a vision-based closed-loop extrusion system showed that the proposed system could self-correct extrusion rates to be within ±10% of the desired rate in less than three seconds.

Figure 4: Examples of Detecting Different Extrusion Conditions Through Developed Vision System (Source: Kazemian et al. [36])

To ensure physical requirements of slate slabs used for roofing are met, Iglesias *et al.* [35] proposed a MV system that returns feedback on whether a slab has surface irregularities, warping, false squaring, material defects, flowerlike staining, and sulphides. The system inspects for these six defects with a camera providing range, grey, and RGB values. Regarding dimensional analysis, the following defects were looked at: material defects, warping, and false squaring. Detection of material defect involved comparing an uncut slab to a theoretical rectangular slab. The two were overlapped and an area difference was used to calculate a ratio and a rectangularity value. Warping was analyzed by cropping the four corners and center of a slab and comparing the mean pixel values of each part. False squaring detection used the assumption that the slabs were cut and square in shape. The algorithm found angles in the slab by considering the corners formed by its edges, and angle deviations from 90º were considered to assess the overall shape quality. The proposed system performed satisfactory in judging the quality of slabs in contrast to human expert graders.

A dimensional measurement MV system was developed by Lee and Yeh [36] for threads in computer numerical control (CNC). A thread contains a set of sinusoidal shaped grooves. The system used inspected the distance from one peak to the next and the depth from peak to root.

Image acquisition was performed on an in-place, cleaned thread. A region of interest (ROI) was defined to reduce image processing, and image correction and filtering followed. Canny edge detection was performed on a binarized image. Using the thread profile and a scale of 6.224 µm per pixel, the researchers achieved measurements with a maximum error of 3.162 µm and a standard deviation of 0.310 µm. In the experiments performed, the system's measured error was under 1% of the actual value.

The case studies and contributions identified demonstrate the variety of applications MV systems have in performing dimensional analyses. Geometric inspections are commonly performed in QC, therefore manufacturers could benefit from extending or replacing outdated methods with the efficiency and reliability of MV systems.

2.3- State Research on Product Surface Analysis

MV systems can provide a nearly thorough visual quality inspection when dimensional analysis is paired with surface analysis. Some useful properties analyzed from the surface of an object is continuity, reflectivity, coloring, and texture. For QC these properties can provide invaluable insight on factors unachievable through dimensional analysis, such as strength of a wall or health of a fruit. Furthermore, surface analysis can be a mere expansion of computational tasks on images already acquired for dimensional analysis. Therefore, as research continues advancing techniques for surface analysis and MV hardware improves, usage of surface analysis will be commonplace in the factories of the future.

Joshi and Patil [37] propose measuring surface texture of hand grinded surfaces using a MV system. The surface is measured on roughness, which is the dependent variable for a linear regression model created. To form the independent variables used for the regression model, a

grey-level co-occurrence matrix (GLCM) is first used to derive surface texture characteristics from an image. A principal component analysis (PCA) is then carried out on the data, and the resulting PCA scores are used as independent variables to regression model. The automated, contactless procedure of the method brings encouragement from the researchers to have it adapted for use on other industrial machining processes.

Wang *et al.* [38] improved surface quality inspection by developing a deep learning model that reduces computational expense. The method developed begins by using a Gaussian filter to reduce noise after image acquisition. The background of images is removed using a Hough transform, which produces a region of interest. Performing background removal allows for reduced processing time in final steps. Finally, a lightweight neural network (NN) is used for feature extraction and defect detection. The NN uses an inverse residual block that effectively reduces the model size and allows the computational burden to be offloaded. The MV system was tested on empty wine bottles, such as in Figure 5. The system could detect defects in the wine bottles at an accuracy of 99.60% and an average inspection time of 47.60 milliseconds per image.

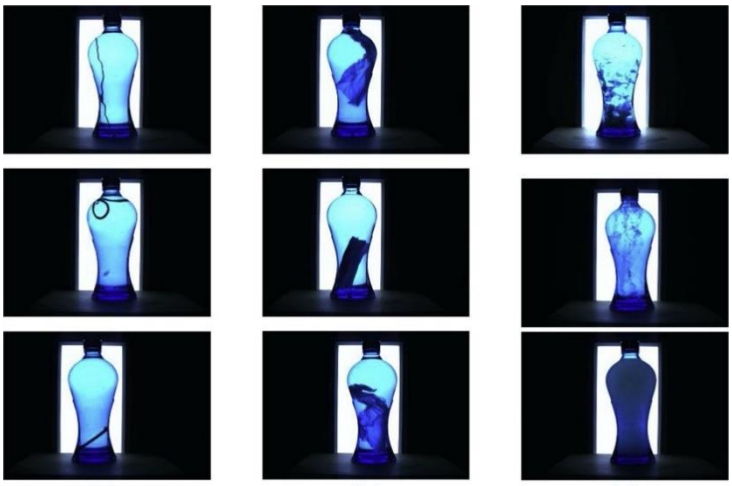

Figure 5: Defect Types a) Small Foreign Matter, b) Large Foreign Matter, c) Contamination (Source: Wang et al. [42])

Friction stir welding (FSW) is a welding technique that uses the friction from a rotating shaft ran against two materials to join them together. A MV system for FSW was developed by Sudhagar *et al.* [39] to inspect a welded surface and classify it as good or bad. The methodology used in developing the system was to perform a greyscale conversion on acquired images, then use the Maximally Stable Extremal Region (MSER) algorithm for feature extraction, and, lastly, classify the images with support vector machine (SVM). An experiment was performed altering parameters, such as weld speed and tool rotational speed, for the welding process and judging the weld quality. Ultimately, it was found that the system could achieve a 95.8% detection accuracy using a linear or quadratic kernel.

In order to determine the tenderness of beef, considered the most important factor in judging the meat's quality, Hosseinpour *et al.* [14] developed a smartphone app that acts as a MV system for this. A textural analysis on the beef surface through gray level co-occurrence matrix (GLCM) provides features that were found to be highly correlated to tenderness. From the extracted textural features, principal component analysis (PCA) was performed. The PCA scores were used to train a Feedforward Multi-layer Perceptron (MLP) neural network (NN) that contained 10-30 hidden layers. The researchers developed a set of algorithms to handle uncontrolled environmental conditions while operating the smartphone. Illumination, rotation, scaling, and translation are factors automatically handled by the created Android app that could normally affect accuracy. In an experiment on thirty unseen beef samples, the app predicted tenderness values (Warner Bratzler shear force) with a mean-squared error, mean absolute percentage error, and coefficient of determination of 3.34, 3.74%, and 0.99, respectively. Besides

providing valuable information on a highly consumed product, the research demonstrates the capabilities of a MV system being mobile and handling robust conditions.

Further contributing to research on produce, Kumar *et al.* [40] achieved a MV system able to classify tomatoes and non-tomatoes, recognize tomatoes ripeness level, and analyze a tomato surface for three possible infections (black spots, cankers, and Melanose). The MV system first performs image acquisition, then feature extraction from which 24 features are extracted. Species classification is done using 14 features and ripeness detection is done using just a mean green feature. Each of the considered tomato infections had specific features used to categorize it. By finding the area of the infection, through a Gabor filter, and using nine other features, the researchers were able to classify infections using a multiclass support vector machine (MSVM). The surface inspection results achieved were 92.31%, 100%, and 92.86% for black spots, cankers, and Melanose, respectively. The proposed method operated with a sufficiently high accuracy and precision when considering the number of features needed by it.

Shin *et al.* [17] devised a MV system to inspect strawberry leaves for powdery mildew (PM), a fungal disease. The researchers used three surface analysis techniques for feature extraction and compared their results: histogram of oriented gradients (HOG), SURF, and gray level co-occurrence matrix (GLCM). Additionally, artificial neural network (ANN) and support vector machine (SVM) were used to classify the features extracted. Ultimately, the best combination of the surface analysis technique and classifier was optimized. The researchers experimented with 254 images and augmented each by rotating it 90º, 180º, and 270º from the original position resulting in 1016 images to be used. Augmenting the images allowed for the experiment to better reflect real-world conditions. Classification accuracy (CA) was primarily concerned in the results, however the researchers did emphasize the elapsed time for each

combination was considered. It was found that the most accurate combination was ANN and SURF, which resulted in a classification accuracy of 94.34% using an image resolution of 908 x 908. The best results for the SVM classification method was with GLCM, which had a classification accuracy of 88.98% using an image resolution of 908 x 908. It was reported that although the HOG and SVM combination resulted in an accuracy of 78.36%, the two are useful for real-time applications because of the drastically smaller processing time required in contrast to the other surface analysis techniques.

Smith *et al.* [41] used the MV technique of photometric stereo (PS) to perform high resolution surface analysis for agricultural weed detection and extermination. PS is a technique developed by Woodham [42], which requires the use of at least three differently placed light sources and a single camera to evaluate the reflectivity of an object's surface. A 3D surface can be reconstructed using this technique and submillimeter detail is achievable, as shown in Figure 6. The researchers argue that PS allows for greater surface inspection abilities over those of an RGB-D device, such as the Kinect, due to reduced complexities in system setup, lessened noise, and greater detail acquisition. To make PS a practical technique for weed extermination, the researchers modified the technique to have it be used on a moving tractor. The modification made was to use only two near-infrared lighting sources, which would not provide sufficient data for 3D reconstruction but enough to target an essential part of a weed. Classification of weeds was accomplished using a support vector machine and neural network. Additional work the researchers suggest using PS for is inspection of potatoes for diseases and damage.

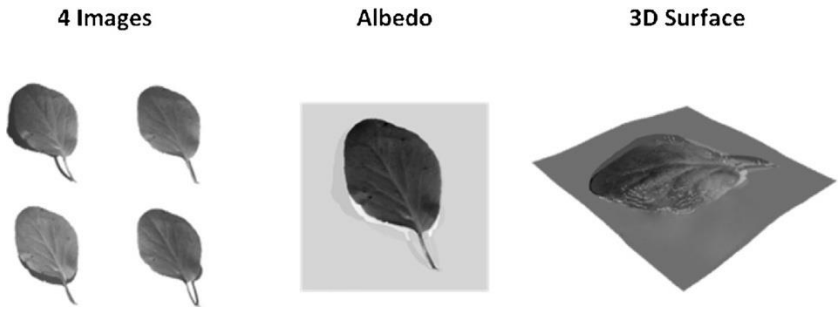

Figure 6: Four Images Acquired Using Different Lighting Sources, an Albedo Image, and a 3D Reconstruction (Source: Smith et al. [45])

Also taking on a precision agricultural problem, Asaei *et al.* [43] developed a MV system to identify tree canopies for precise pesticide spraying. The intricate electromechanical system used LabVIEW for real-time identification of treetops. Once a green color threshold was exceeded, the researchers used 10%, this indicated that sufficient greenage was in the camera view and the spraying system should be activated. In a field test, the researchers used the MV system to spray water, acting as pesticide, on water sensitive paper (WSP). Measurements from the WSP were calculated using an image processing toolbox in MATLAB. To do this RGB images of the WSP were acquired and converted to the HSV color space, where the hue component was only considered to segment droplets from the images for counting and area sizing. The results showed that at all speeds the system was tested moving through the field it could lead to at least a 54% reduction in pesticide spraying.

Zhuang *et al.* [44] advanced the detection of citrus fruits by MV systems to accelerate the process toward fully automated harvesting. A monocular vision system using the visible light spectrum could identify mandarins growing individually or in clusters. The proposed system acquired images that were preprocessed using the block-based local homomorphic filtering algorithm, which compensated for non-uniform illumination. Adaptive enhanced RG chromatic mapping was then used to further increase contrast in the foreground and background of images.

Clustered fruits were separated using the MCWT method, which identified each fruit by a different color. Trouble with over-segmentation was taken care of by the convex hall operation. An LBP, a local texture descriptor, was used as the input for a support vector machine (SVM) classifier. The proposed system had a recall of 0.862 and a detection speed of 1.9 fps.

Kumar and Kumar [45] explored the surface roughness (R_a) estimation quality of a MV system when varying light colors were used. In the experiment conducted, yellow, white, and blue light were used to illuminate 12 objects 3D printed with ABS material. After image acquisition and preprocessing, five Grey Level Co-Occurrence Matrix features were extracted from the images. Using entropy, contrast, correlation, energy, and homogeneity as inputs, an artificial neural network (ANN) was created to predict surface roughness. The quality of the output by the ANN was compared to the output of a dedicated surface roughness measuring device. The results of the experimented showed that the blue light had the greatest correlation (0.7906) between the ANN prediction and the measuring device. The yellow light had a correlation of 0.4573 and the white light has a correlation of 0.3525. The researchers propose further experimentation with other light colors and material colors.

The identified contributions on surface analysis showed how MV systems are being used to study textures, colors, and patterns on products. Manufacturers are gaining insight on important textural features through the non-destructive use of MV. Additionally, achieving color accuracy in production processes is making headway with MV systems, as is the use of precise color identification.

2.4- Literature Discussion

Table 1 summarizes the applications and techniques of the literature considered in this chapter.

Analysis Type	**Application Domain**	**Techniques Used for Digital Quality Control**
Product Free-Form Analysis	Natural products and leather cutting examination	Polygonal curve deviation using Single-segment and Multiple-segment
	Inspection of micro-milling tools	Root mean square deviation (RMSD), Exponential transform, Infinite symmetric exponential filter
	Inspection and optimal parameter identification in alloys	Taguchi technique, Blob analysis
	Sorting and recycling of non-ferrous materials	PCA-SVM, Response surface methodology, Numerical simulation
	Agricultural produce deformities inspection	Linear regression, Oval Difference Degree, Grid Calculation, Hollow detection
	Tracking and processing livestock	Convolutional Neural Network (CNN), Rotation, scale, and translation augmentation techniques
	Identifying fatigue cracking in metallic compounds	Deeply Supervised Object Detector, YOLO algorithm, Single Shot MultiBox Detector, DenseNet algorithm
	Inspection of microscale e-jet printing	Blob analysis, Otsu thresholding algorithm, Morphological operations: erosion and dilation
	Automate produce harvesting	Fully Convolutional Network, Blob analysis, Stereo image analysis
	Examination of construction steel frames	Hough Transform, CED, Harris corner algorithm

Product Dimensional Analysis	Determining precise measurements of industrial equipment	Subpixel edge detection, CED, Otsu thresholding, Taguchi method, Least squares regression
	Agricultural produce deformities inspection	CED, Sobel edge detection, Support Vector Machine (SVM), Median filter
	Inspection of alcoholic bottle quality	Fourier transform, Blob analysis, Least square circle fitting, Edge points double classifying
	Examination of additive manufacturing for construction	Otsu thresholding, Blob analysis
	Inspection of slate slabs	Texture analysis, Local binary pattern methods
Product Surface Analysis	Texture characterization for grinded surfaces	Grey level co-occurrence matrix (GLCM), Principal component analysis (PCA), Multiple regression analysis
	Inspection of wine bottles	Hough transform, CNN, Depthwise convolution and pointwise convolution
	Examination of friction stir welding	Maximally stable extremal region algorithm, SVM
	Analysis of beef tenderness via a mobile system	Rotation, scale, and translation augmentation techniques, GLCM, Feedforward Multi-layer Perceptron neural network, PCA
	Agricultural produce deformities and disease inspection	Top hat filter, Gabor wavelets, Multiclass SVM, Histogram of oriented gradients, Speed-up robust features, GLCM, Neural Network
	Agricultural field and garden inspection	SVM, CNN, Homomorphic filtering, Convex hull operation, Histogram intersection kernel, GLCM

Table 1: Categorization of Product Quality Inspection Techniques Across Various Application Domains

QC systems using MV are shaping the future of how product inspection will be performed. The research contributions highlighted in this chapter describe the success contemporary systems are having in efficiently, accurately, and consistently performing inspection tasks. The progress achieved in identifying new techniques and improving already existing techniques for digital quality inspection systems is at par with human abilities or better, and indicative of a complete supersession in the years to come. In nearly all cases, the reported work attained results that were satisfactory in product inspection tasks. If the ultimate state of a system was undesirable, it nonetheless led to ideas and suggestions of where future work could be directed for improvements.

Machine learning was commonly used in the reported systems for its classification and identification abilities. However, a repeatedly mentioned limitation of using ML techniques was the lack of training data available to improve classification accuracy and generalization. The expectation is that overtime the available datasets will improve in quantity and quality, thereby enhancing the performance of the methods used. The two most used ML models were support vector machines (SVM) and neural networks (NN), specifically convolutional neural networks (CNN). The former model is a classification method that constructs a hyperplane through a set of data in p-dimensions. This separation technique is used for final quality classification and in combination with other models in quality inspection systems. CNN is a deep learning class that has grown to be widely used for imagery analysis due to its speed and low error rates. When learning, this multilayer NN extracts features from images that allow it to accurately execute MV tasks without the need for manual feature training. CNN is primarily used for quality classification.

Another important challenge that continues to be explored is the versatility of quality inspection systems under uncontrolled environmental conditions. Some of the MV systems used were designed with an intent to operate outdoors where inconsistent lighting is one of many environmental factors that can affect output validity. While significant consideration was given to overcome these problems, there remains a need to improve robust handling. Furthermore, present and future inspection product inspection systems could benefit from having highly dependable rotation, scale, and translation augmentation techniques. Such improvements could increase the number of mobile inspection systems, as was demonstrated by Hosseinpour et al. [14], or assist with handling vibration and movements in factory settings.

Evidently the use of MV systems is permeating through a wide range of manufacturing processes. The scale of the developed inspection systems is both at a micro level, such as the microscale e-jet printing inspection by Lies et al. [27], and at a macro level, as in the examination of large-scale additive manufacturing for construction by Kazemian et al [36]. Food manufacturing processes such as rice quality inspection (Chen et al. [33]) are benefitting from MV systems agility. Underdeveloped processes such as the recycling of nonferrous metals (Wang, Chao et al. [21]) are growing in efficiency and reliability using MV systems. Some researchers have already presented nearly autonomous systems that are able to act in a variety of ways based on the perception of their system, such as the kiwi harvester (Williams et al. [28]) and trout processor (Azarmdel et al. [25]). Continuously advancing equipment and techniques are sure to further expand the scope of issues and complexities to which MV systems can be used for in product quality inspection.

2.4.1 Discussion on Free-form Analysis

A product inspection system is categorized as being able to perform free-form analysis if its inspection tasks dealt with analyzing products of complex forms or having complex areas. As summarized in Table 1, several techniques were utilized to perform product inspection across domains for multiple applications. Common throughout the free-form analysis literature is contrasting the detected area/shape of a product to that of what it should be, such as leather hide inspection system developed by Pacella et al [19]. Additionally, the Otsu thresholding method is observed to be commonly used in the free-form analysis techniques to distinguish the foreground and background of images. Analysis of complex forms is greatly facilitated by this thresholding technique that binarizes images in a computationally efficient manner. Lastly, blob analysis was used in several papers to obtain the form of an item under inspection. Blob analysis extracts the contour for an item of interest based on a specified grey-scale pixel intensity range. Once a blob is determined, information on the subject can be determined, such as perimeter or area in pixels. Conversion from pixels to distance can be determined through calibration. Blob analysis provides a relatively simple method for finding the 2D shape of an item.

2.4.2 Discussion on Dimensional Analysis

The literature concerning dimensional analysis for product quality inspection largely used Canny edge detection and in a single case, Sobel edge detection. Canny edge detection is a popular computer vision algorithm that uses calculus of variations to achieve lower error rates and denoising functionality. Part of the Canny edge detection algorithm is using a Gaussian filter, a commonly used technique to provide necessary smoothing in an image.

2.4.3 Discussion on Surface Analysis

A popular approach for textural analysis is the use of a grey level co-occurrence matrix (GLCM) to extract features over a surface. Features such as contrast, correlation, energy, and homogeneity can be used as inputs for machine learning models. An example of this is the characterization of surface texture in hand grinded surfaces as illustrated by Joshi and Patil. Color analysis, a form of surface analysis is also greatly used. Closely examining color values is critical to much of the agricultural and food related product inspection, such as the mature mandarin detection system developed by Zhuang et al. [48] where an adaptive enhanced red/green chromatic mapping was used to identify the ripe citrus food for harvesting.

2.4.4- Algorithms Observed

A brief overview of commonly used algorithms is provided in the following paragraphs. Taguchi method (or technique) consists of statistical methods developed for QC in manufacturing. The methods developed use a monotonic loss function if the production situation is improved by exceeding or falling below a target, or a square-error loss function if the production situation requires a strict target be met. Taguchi methods have expanded since their development to other areas of engineering.

Principal component analysis is a dimensionality reduction technique applied to datasets and commonly used in ML. By dimensionally reducing a dataset, analysis is simplified at the cost of some accuracy. PCA is performed by first standardizing all variables in the data to a range of 0 to 1. Next, a covariance matrix is calculated for all the used variables, which based on the covariance sign value can indicate how two variables are correlated. Following this the eigenvectors and eigenvalues are computed to identify the principal components. The eigenvalues calculated from the covariance matrix indicate the significance of each principal

component. Lastly, only the most significant eigenvectors can be selected in a feature vector to achieve dimensionality reduction. Using the feature vector, the original data is recast to meet the dimensionality formed by the principal components.

Support vector machine (SVM) is a ML technique used for classification. The technique is an example of supervised learning that attempts to find a hyperplane that passes through two classes. The hyperplane may pass through high-dimensional space to separate two classes. Once the hyperplane is determined, a new input can be classified based on where it is relative to the hyperplane. The hyperplane is generally designed to have the greatest distance between the two classes to improve its generalization.

A convolutional neural network (CNN) is a deep neural network class mostly used for image analysis. CNN are a multilayer perceptrons prone to overfitting data but there are ways to prevent this. A significant advantage of using CNN is that the network filters are determined through the automated learning as opposed to manually determining them through traditional methods. CNN's excellent performance has led to its use in numerous applications.

Grey-level co-occurrence matrix is an image processing method used for textural analysis in an image. The method relies on comparing pixel intensity values to make a quantified judgement on how an item in an image may be texturally. In addition to the applications presented in this literature survey, this method is often used for medical image analysis.

Considering the problem statement of this thesis calls for a robust and adaptable system that can perform dimensional and surface inspections, the literature reviewed showed blob analysis could be used to accomplish that. The literature on free-form analysis presented how blob analysis is used to inspect the varying shapes and sizes produce can come at, the literature on dimensional analysis presented how blob analysis is used to determine the dimensions of

bottles, and the literature on surface analysis showed blob analysis is used to identify defects on wine bottles. Therefore, blob analysis serves as a useful technique in accomplishing the goals of this work.

CHAPTER III

PROPOSED MACHINE VISION SYSTEM

The developed QC system consists of a 5MP, CMOS industrial camera made by Hikvision, a circular LED light source, and a metal rig (Please see Figure 7).* The LED light source allows for the light intensity to be adjusted from off to peak brightness. The metal rig is approximately 17.5 x 8.5 inches and allows for a robotic arm to be interlocked in the rig. The modular design of the rig provides a convenient and precise way to use a robotic arm in the QC system.

Figure 7: Machine Vision Setup Used.

* The work illustrated in Chapters 3 and 4 is featured in the Complex Adaptive Systems Conference 2021. Aditya Akundi and Mark Reyna, A Machine Vision Based Automated Quality Control System for Product Dimensional Analysis, 2021.

Image processing is performed on the Dobot Vision Studio application which provides a simple interface to operate on and organized feedback on data processed. Blob analysis is an example of an image processing technique used on Dobot Vision Studio largely used in this thesis. Dobot Vision Studio allows for multiple hardware devices to connect and communicate with each other, which is shown with the robotic arm in Chapter 6. The computer running the Dobot Vision Studio application is a Dell Inspiron with an i7 10^{th} generation processor and 16 GB of memory.

CHAPTER IV

PRODUCT INSPECTION BASED ON DIMENSIONAL ANALYSIS

The algorithm used in the proposed QC system compares the dimensional likeness of similar products (i.e. products of the same geometric shapes).* An overview of the algorithm (Figure 8) is provided:

1. First, perform an inspection on an exemplar object known to meet the desired design specifications.
2. Store parameter data from the qualified object for future comparison.
3. Iterate a loop indefinitely, or a specified number of times, with each iteration performing an inspection on a new object. The data collected from each new object is compared to the initial object and given a percent rating on its likeness to the initial object. A new object is considered acceptable if it lies within a specified tolerance.

The dimensional inspection process is currently designed to analyze the surface of an object from a top view. This process is considered robust for its handling of complex shapes and geometries. Examples of shapes capable of analysis are sinusoidal objects, gapped objects, and objects with varying edge patterns. The dimensional inspection process performs a blob analysis which

* The work illustrated in Chapters 3 and 4 is featured in the Complex Adaptive Systems Conference 2021. Aditya Akundi and Mark Reyna, A Machine Vision Based Automated Quality Control System for Product Dimensional Analysis, 2021.

extracts the contour of a surface in an image [8]. The blob analysis uses a single threshold mode, a light blob to dark background polarity, and a minimum object pore area of 100 pixels in a 1600 x 1600 image. The object under inspection can be placed anywhere within the area captured in an image and can be rotated any degree about an axis orthogonal to the base and camera. No loss in accuracy results from these translations and rotations. Additionally, the average run time for the proposed algorithm is 266 ms per item after the delay for object replacement has been removed, which improves upon the speeds of the 0.5 s time in the work by Zhang et al [6]. Using a calibrated camera, the system can output the physical distance of a surface's perimeter and area. Therefore, if an object known to meet the desired physical design specifications is available, it can serve as the initial object for the algorithm considered. If no initial object is available, the expected parameter values can be manually inputted. The algorithm provides a strong comparison of how a set of products appears relative to a base. Four parameters are considered in the algorithm's likeness scoring: 1) perimeter, 2) area, 3) rectangularity, and 4) circularity. The perimeter is measured as the number of pixels in an object's outline contour. Computing the perimeter is as follows,

$$Perimeter = \sum_{m=1}^{width} \sum_{n=1}^{length} pixel\_contour(m,n) \qquad \textit{Equation 1}$$

, where width and length can be determined from the image size and the *pixel_contour* function returns a 1 or 0 if the pixel is on the contour (1) or not (0), respectively. Similarly, area is measured as the number of pixels contained in an object. Computing the area pixel count is as follows,

$$Area = \sum_{m=1}^{width} \sum_{n=1}^{length} pixel(m,n) \qquad \textit{Equation 2}$$

, where the *pixel* function returns a 1 or 0 if the pixel is in the blob or not, respectively. Rectangularity measures the area filled by the object over the area filled by the smallest

circumscribed rectangle containing the object and outputs a value from 0 to 1, where 1 is a pure rectangle (Equation 3). Likewise, circularity measures the area filled by the object over the area filled by the smallest circumscribed circle containing the object and outputs a value from 0 to 1, where 1 is a pure circle (Equation 4).

$$Rectangularity = \frac{Area_{filled}}{Area_{SCR}} \qquad \textit{Equation 3}$$

$$Circularity = \frac{Area_{filled}}{Area_{SCC}} \qquad \textit{Equation 4}$$

, where in equation 3 $Area_{filled}$ is the area filled by the product and $Area_{SCR}$ is the area filled by the smallest circumscribed rectangle over the product. Likewise, in equation 4 the $Area_{filled}$ is the area filled by the product and $Area_{SCC}$ is the area filled by the smallest circumscribed circle over the product. These four parameters can simultaneously be measured and are expressed in the likeness score as shown in equation 5.

$$L = aP + bA + cR + dC \qquad \textit{Equation 5}$$

Where, a, b, c, and d, are weights assigned to prioritize parameter values. P, A, R, and C are respectively, the perimeter, area, rectangularity, and circularity. These values are calculated using equation 6.

$$X = 1 - \frac{|x_{new} - x_{initial}|}{x_{initial}} \qquad \textit{Equation 6}$$

Where x_{new} can be substituted with a parameter from a product being compared and $x_{initial}$ can be substituted with a parameter from a desired product. Finally, the QC system determines whether a product inspected should be accepted or rejected based on product geometrical similarity. This decision is based on a predetermined threshold that can be altered to be highly selective or more tolerable.

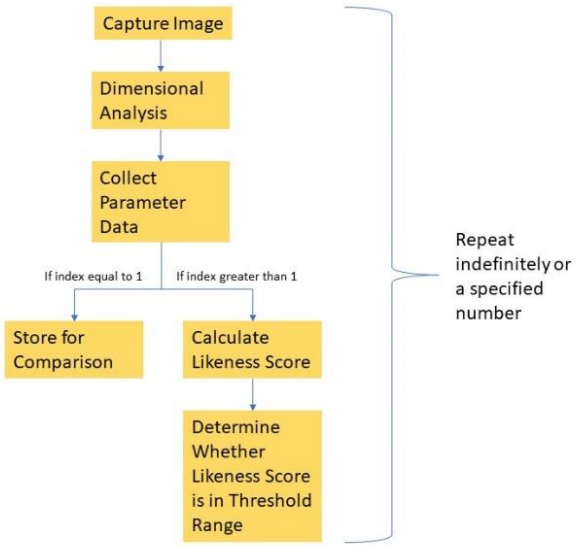

Figure 8: Proposed Machine Vision Algorithm for Product Dimensional Analysis

A step-by-step process flow of the algorithm is provided here:

1. Capture a grayscale image of an initial item that best meets the quality requirements.
2. Perform dimensional analysis on the image in step 1.
3. Store parameter data values for future comparison use.
4. Capture image of new item.
5. Perform dimensional analysis on image from step 4.
6. Using parameter data in step 5, calculate likeness score for an item.
7. Check if likeness score is within threshold range (a greyscale intensity value from 0 to 255). Output result for proper item handling.
8. Repeat steps 4-7 a desired number of iterations.

4.1- Initial Test Results and Discussion

4.1.1- Common Shapes

To test the performance of the proposed QC system, three common shapes were used: cubes, cylinders, and sinusoids (Figure 9). The items tested were printed using MakerBot 3D

printers, which allowed for rapid dimensional alterations. Data collected from several cube test comparisons is shown in Table 1. The base items are those that would be test standards and the tested are those compared to the base. As shown in Table 1, the likeness scores obtained when comparing two dimensionally different objects are low. Furthermore, when observing the likeness scores of dimensionally equal objects, a perfect or near-perfect likeness score is obtained.

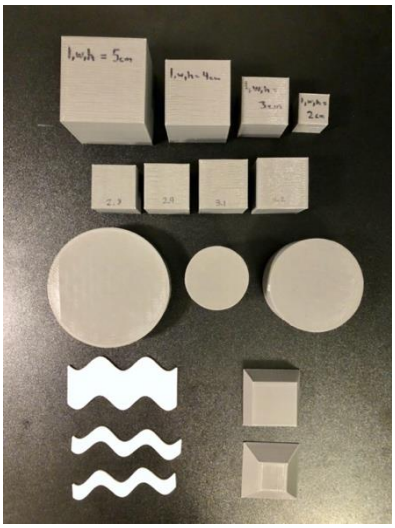

Figure 9: Shapes Used for Testing

Shape	**Base**	**Tested**	**Likeness Score**
Cube	5 cm	5 cm	1.000
Cube	5 cm	4 cm	0.794
Cube	4 cm	3 cm	0.740
Cube	3 cm	2 cm	0.678
Cube	2 cm	2 cm	0.999

Table 2: Cube Test Comparison

An example of the full data used to calculate the likeness score for base 4 cm and tested 3 cm in Table 1 is shown in Table 2. Note that the values shown in the table are in pixels and have not been converted to distance. Additionally, the coefficients a, b, c, and d used for the likeness score are 0.4, 0.4, 0.1, and 0.1, respectively. These values were selected to prioritize perimeter and area in making a quality decision. In the case that an item contains the same perimeter and

area but not shape as an intended item, the rectangularity and circularity scores can flag this unique instance.

Item	Area	Perimeter	Circularity	Rectangularity
Cube 4 cm	173503.000	1780.497	0.647	0.985
Cube 3 cm	92641.000	1297.453	0.638	0.984

Table 3: Test Case Data

Data on the tests performed for cylinders and sinusoids is provided in Table 3 and Table 4. In Table 3, r is the radius of the cylinder and h is the height of the cylinder. In Table 4, l is the length of the sinusoid and w is the width of the sinusoid.

Shape	Base	Tested	Likeness Score
Cylinder	r = 4 cm, h = 2 cm	r = 4 cm, h = 2 cm	0.999
Cylinder	r = 4 cm, h = 2 cm	r = 3 cm, h = 3 cm	0.771
Cylinder	r = 3 cm, h = 3 cm	r = 3 cm, h = 3 cm	0.999
Cylinder	r = 3 cm, h = 3 cm	r = 2 cm, h = 4 cm	0.701
Cylinder	r = 2 cm, h = 4 cm	r = 2 cm, h = 4 cm	0.999

Table 4: Cylinder Test Comparison

Shape	Base	Tested	Likeness Score
Sinusoid	l = 1 cm, w = 7.5 cm	l = 1 cm, w = 7.5 cm	0.995
Sinusoid	l = 1 cm, w = 7.5 cm	l = 0.8 cm, w = 7.1 cm	0.099
Sinusoid	l = 1 cm, w = 7.5 cm	l = 2.5 cm, w = 7.5 cm	0.948

Table 5: Sinusoid Test Comparison

4.1.2- Complex Shapes

A complex shape inspection was performed to demonstrate the proposed QC system's capabilities. The complex shape used contains a single point edge, a squared-bumps edge, a circular-bumps edge, and a triangular-bumps edge. Figure 10 shows the image results of the inspection between a base complex part with a 7 cm inner square reaching each corner and the base part shrunken by 95%. Additional inspections and data are provided in Table 5, showing how the system performed with the same base part against an alike part and an enlarged part.

Shape	Base	Tested	Likeness Score
Complex Part	Inner square = 7 cm	Inner square = 7 cm	0.996

Complex Part	Inner square = 7 cm	Base shape • 0.95	0.948
Complex Part	Inner square = 7 cm	Base shape • 1.05	0.949

Table 6: Complex Part Test Comparison

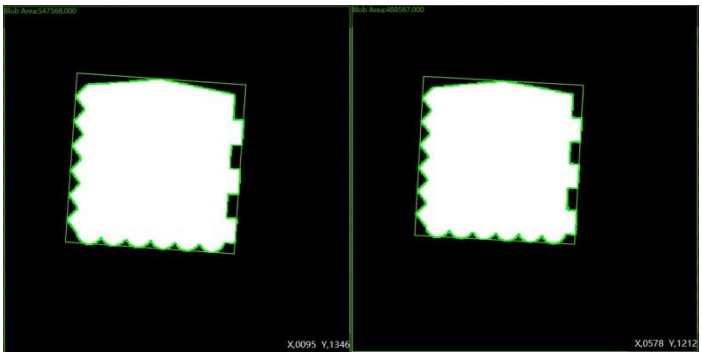

Figure 10: (a) Original Complex Part; (b) Complex Part Shrunken to 95%

4.1.3- Frustums

Although the QC system proposed performs well for items with entirely uniform cross-sections, the system at its current stage is unable to properly inspect items that have varying cross-sections. An example of this shortcoming is the frustrum shape, which is like a pyramid that has had its upper section sliced. The inspection system misidentifies the top surface with the larger bottom surface, therefore reports incorrect data.

4.1.4- System Accuracy

To demonstrate the inspection capabilities of the proposed system, a test was performed using four cubes with slightly varying dimensions to the base. The base cube's sides are 3 cm, while the tested cubes have sides of 2.8 cm, 2.9 cm, 3.1 cm, and 3.2 cm. The test results are shown in Table 6 and the blob analysis for the tested 3.1 cm cube is shown in Figure 11. The likeness scores in Table 6 demonstrates the system's capacity to identify millimeter-level defects. In application, a high likeness score threshold can be set to avoid even minor dimensional deviations.

Shape	**Base**	**Tested**	**Likeness Score**
Cube	3 cm	3 cm	1.000

Cube	3 cm	2.8 cm	0.924
Cube	3 cm	2.9 cm	0.958
Cube	3 cm	3.1 cm	0.958
Cube	3 cm	3.2 cm	0.923

Table 7: Cube Test with Minor Dimensional Changes

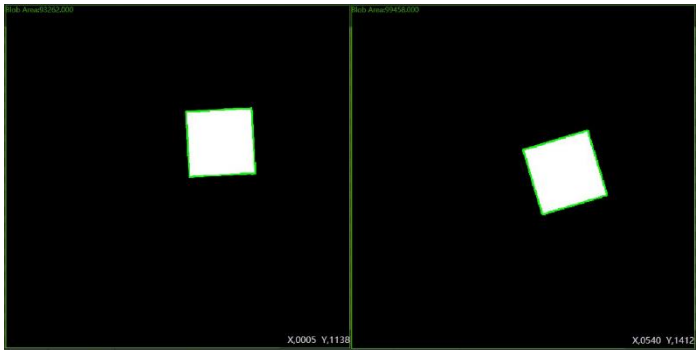

Figure 11: (a) Dimensional Analysis 3 cm Cube; (b) Dimensional Analysis 3.1 cm Cube

CHAPTER V

PRODUCT INSPECTION BASED ON SURFACE ANALYSIS

The goal of surface analysis in this thesis is to identify areas on an object's surface that are outliers in coloration with respect to the entirety of the object. Examples of surface defects that result in dissimilar coloration on a surface are dents, bumps, scratches, and material errors in producing the product (e.g., burning or overstretching the material). Identifying surface defects in quality control is important to ensuring the desired aesthetics and functionality of a product are met. As mentioned in the introduction, a product failing to meet the desired aesthetics will be unattractive, possibly resulting in reduced sales. Functionally, a surface defect will indicate a product's design has not been perfectly met, which could mean its mechanical integrity is corrupted. A functional failure could have dire consequences, as in the case of a vehicle break failure, therefore incorporating surface analysis in QC could be worthwhile in decreasing such failures.

5.1- Hardware and Algorithm

MV is naturally advantageous for the mentioned surface analysis concerning coloration since colored images are inspected. The surface analysis in this work uses grayscale images that are 1600 x 1600 pixels. The QC system used for surface analysis operates with the same equipment and software for dimensional analysis in Chapter 4. Furthermore, the same images

used for dimensional analysis can be used for surface analysis. Therefore, placement of an item on the rig can be anywhere in the area captured in an image and be rotated in any way about the axis orthogonal to the rig and camera. The dimensional and surface analyses operating on exact copies of the same image helps reduce the overall inspection time. Additionally, the two analyses can be performed asynchronously in the same inspection flow since the same image is used and both analyses are independent of each other.

There are two assumptions made about the product being inspected. The first is that the item contains a surface that is uniform and smooth. Uniform meaning that all points on an item are expected to appear the same in color. Smooth meaning that all points on an item are at the same level and no points are higher or lower relative to one another. For example, if the top surface of a white cube were inspected, then the assumption for inspection is that this surface is uniformly the same white color, as seen by the camera, and that all points on the surface are equidistance from a plane parallel to the camera lens. If this assumption is not met in the design of an item, then the system will classify nonuniform or varying height points as defects.

The second assumption is that all pores in a design are in the specified area range, a range of pixels considered for area. Unlike the dimensional analysis algorithm in the previous chapter, the surface analysis algorithm does not compare the item under inspection to a provided base item. Instead the algorithm is designed to predict the intended design of an item by filling pores within an area range. This step attempts to remove any defects from an item and use this design for comparison. Blob analysis is used for both the predicted surface and the given surface. By using blob analysis an acceptable minimum pore area can be specified. Pores are defined here to be any touching pixel groups below the pixel intensity threshold found within items bodies. For example, the hole in a ring would be a group of pixels falling below the intensity threshold,

therefore would be categorized as a pore. Adjusting the minimum pore size is important in limiting noise during inspection and is part of what is done to prevent noise in the presented system. For the blob analysis attempting to identify defects, the minimum pore area is 300 px. Meaning any defects or designed pores under 300 px will be filtered and not identified. Meanwhile, the blob analysis attempting to predict the design of an item has a minimum pore area of 10,000 px. Setting a large minimum pore area removes most defects on a surface by filling any pores (noise or defects). While setting a large minimum pore area allows a surface to be predicted, it has the drawback of considering large defects (defects exceeding 10,000 px) as part of the intended design. Conversely, any designed pore that is under 10,000 px will be identified as a defect. The detectable surface defects are therefore 300 px on the lower bound and 10,000 px on the higher bound. Any desired pores in an item must be greater than 10,000 px. The lower bound (300 px) and upper bound (10,000 px) can be easily modified to better suit an inspection task. However, reducing the lower bound increases the system's probability of identifying noise as a defect. Increasing the upper bound allows for larger defects to be identified however requires that designed area pores in an item be greater than this new upper bound. The lower and upper bound were experimentally determined. A summary on how the system treats pores is provided in Table 7:

Pixel Area	**Classification**
< 300 px	Pore is treated as noise.
> 300 px and < 10,000 px	Pore is treated as defect.
> 10,000 px	Pore is treated as design.

Table 8: Summary on Surface Analysis Pore Classification

An overview of the surface analysis algorithm is as follows:

1. An image of an item is acquired in greyscale format.

2. The image is enhanced to improve desired quality characteristics.
3. The image is filtered to smooth coloration.
4. Two blob analyses are performed. One estimating how the item under inspection would appear without defects and the other blob analysis identifying defects on the surface.
5. The difference in acceptable area (area not defective) is determined and a decision is outputted.

The enhancement made to an image in step two is as follows. The greyscale image captured in step one will undergo sharpness enhancements. The sharpness enhancement contains two parameters, sharpness intensity and kernel size. The sharpness intensity value ranges from 0 to 1,000 where increasing this value sharpens the image. The kernel size ranges from 1 to 51 and decides the size of sharpness area. The sharpness intensity and kernel size used for the system are 550 and 30, respectively. Both values were experimentally determined to adequately sharpen the edges of an object while not sharpening edges of a defect.

The filtering done to an image in step three is as follows. Once the enhanced image in step two of the algorithm is passed to step three, a Gaussian filter is used to suppress noise by smoothing pixels. The Gaussian filter is an important pre-processing step that considers a pixel and its neighbors, then based on a Gaussian filter kernel size makes the specified changes. The Gaussian filter kernel size ranges from 1 to 51 and increases images smoothness as its value increases. This technique blurs an image which reduces pixels with outlying color intensities due to noise. The Gaussian filter kernel size used is 6 which was experimentally determined.

The design and rationale in step four were previously described in assumption two for surface analysis. The blob analysis predicting an item’s surface in step four returns an image

with all pixels evaluated to be acceptable. The blob analysis inspecting an item for defects returns an image like the blob analysis predicting the surface, however the pixels that are included in defective areas are excluded. Both returned images set all recognized pixels (those that are acceptable on the surface or predicted to be) to the max greyscale intensity of 255 (white) and all other pixels to the minimum intensity of 0 (black). With both images containing binary pixels, the white pixel count can be determined for each image and then compared. This comparison is step five in the algorithm and based on the difference the system will decide whether the surface is acceptable (no defects found) or defective (one or more defect found). An example of an image captured by the QC system with a defect and the conversion to binary pixels for predicted and given is shown in Figure 12.

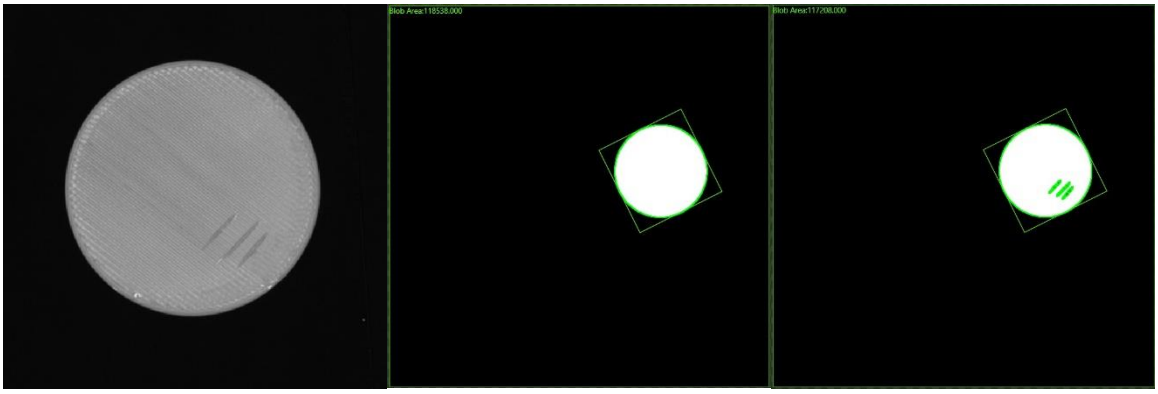

Figure 12: Defective Item a) Unprocessed Image, b) Predicted Surface, c) Surface with Defects

The reason for choosing to compare an item against a predicted design of itself is, as opposed to a base model, is to reduce noise in the comparison. The presented surface analysis technique uses the same image for the blob analyses, therefore noise in this image is filtered out or shown in both images (a comparison would show no difference due to noise). If a base model were used, then two separate images are required, each with some noise. Furthermore, if image used for the base model contains significant noise, this could lead to poor comparisons the

remainder of the inspection procedure. Also, the difficulty of balancing an acceptable level of noise and the smallest detectable defects grows with the base model comparison.

5.2- Test Results

The surface analysis performance of the proposed QC system was assessed through a series of inspections on 3D printed wafers. These wafers are 40 mm in diameter and 1.5 mm in height with a white surface. The wafers inspected either contained a surface with no defects, manually created defects, or defects printed in the design. The goal of these tests was to demonstrate how the QC system identifies plausible defects in manufacturing as well as its ability to handle any type of defect.

5.2.1- Wafers with No Defects

The test results on wafers with no defects is shown below as well as the image output for several trials.

Trial	Item	System Result	Number of Detected Defects	Actual Number of Defects	Area of Predicted Item	Area of Examined Item
1	Wafer with no defects	Acceptable	0	0	117380	117380
2	Wafer with no defects	Acceptable	0	0	117405	117405
3	Wafer with no defects	Acceptable	0	0	117537	117537

Table 9: Test Results on Wafers with No Defects

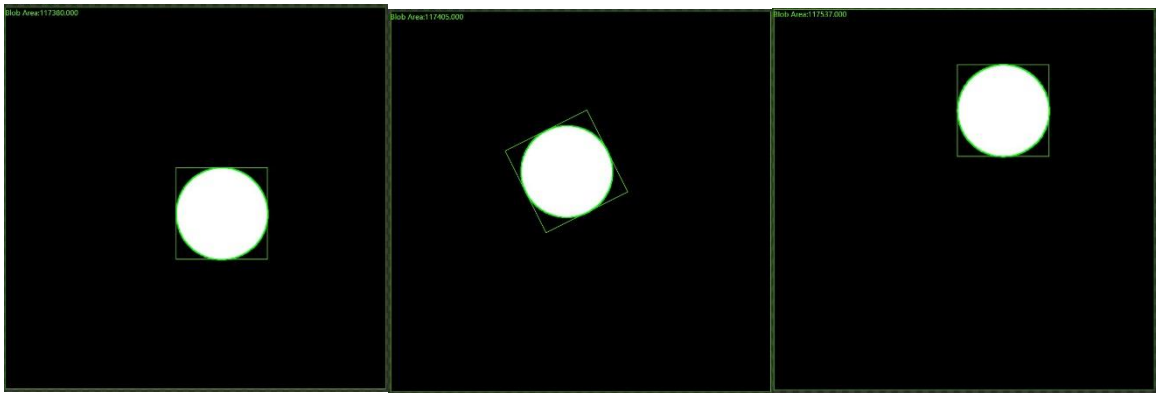

Figure 13: Output Images for Wafer with No Defects (Trials 1-3)

Each trial was performed the same way except for the location the wafer was placed on the inspection area. Varying the location of the wafer was done to demonstrate the system's output will remain the same regardless of item location. In each trial the expected number of defects was 0 and the number of defects found was 0. These trials demonstrate the system's ability to correctly output no defects when there are none.

5.2.2- Wafers with Plausible Defects

The test results on wafers with plausible defects is shown below as well as the image output for these trials. These defects were either created manually with a tool or printed in the item. The item name provides a short description on the defect created. More information on how the defects appear is provided below.

Trial	Item	System Result	Number of Detected Defects	Actual Number of Defects	Area of Predicted Item	Area of Examined Item
4	Wafer with box cuts	Defective	3	3	118538	117208
5	Wafer with box cuts	Defective	3	3	118100	116739
6	Wafer with box cuts	Defective	3	3	118361	117147
7	Wafer with 0.5 mm bump	Defective	1	1	117177	112346
8	Wafer with 0.5 mm bump	Defective	1	1	116832	111992

9	Wafer with 0.5 mm bump	Defective	1	1	117116	112243
10	Wafer with 1 mm bump	Defective	1	1	117280	112402
11	Wafer with 1 mm bump	Defective	1	1	116870	1120.03
12	Wafer with 1 mm bump	Defective	1	1	117007	112095
13	Wafer with continuous marker dots	Defective	11	11	117688	113644
14	Wafer with continuous marker dots	Defective	11	11	117317	113252
15	Wafer with continuous marker dots	Defective	11	11	117472	113394
16	Wafer with screw dents	Defective	3	3	118348	115876
17	Wafer with screw dents	Defective	4	3	117992	115965
18	Wafer with screw dents	Defective	4	3	118363	116289
19	Wafer with long scratch	Defective	1	1	118546	116164
20	Wafer with long scratch	Defective	3	1	118121	116268
21	Wafer with long scratch	Defective	2	1	118591	117155
22	Large marker blob	Acceptable	0	1	997000	997000
23	Large marker blob	Acceptable	0	1	99880	99880
24	Large marker blob	Acceptable	0	1	99611	99611

Table 10: Test Results on Wafers with Manually Created Defects

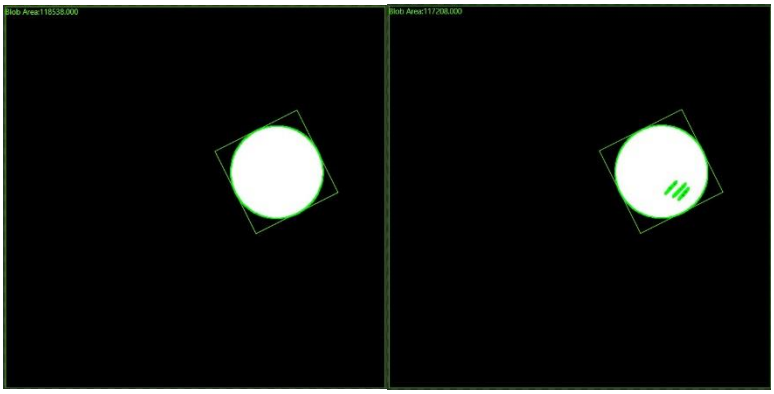

Figure 14: Trial 4- Box Cuts (Predicted and Tested)

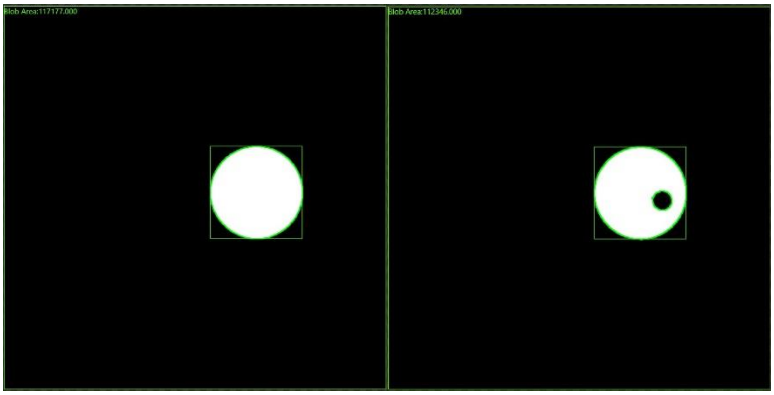

Figure 15: Trial 7- Wafer with 0.5 mm Bump (Predicted and Tested)

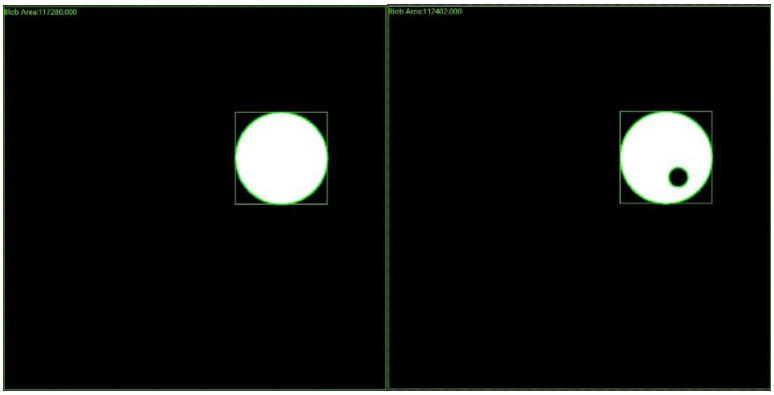

Figure 16: Trial 10- Wafer with 1 mm Bump (Predicted and Tested)

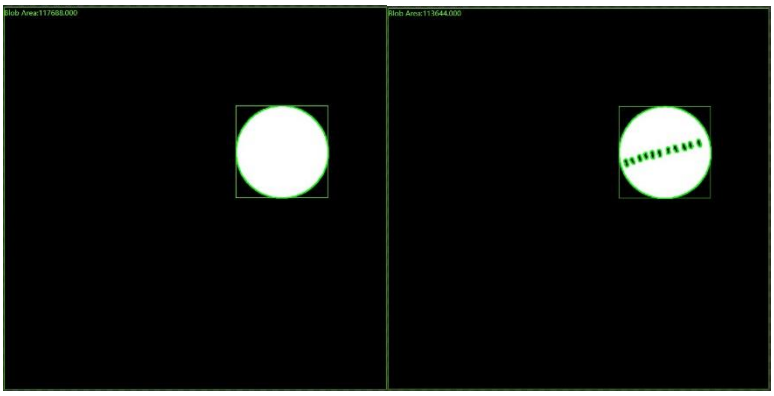

Figure 17: Trial 13- Wafer with Marker Dots (Predicted and Tested)

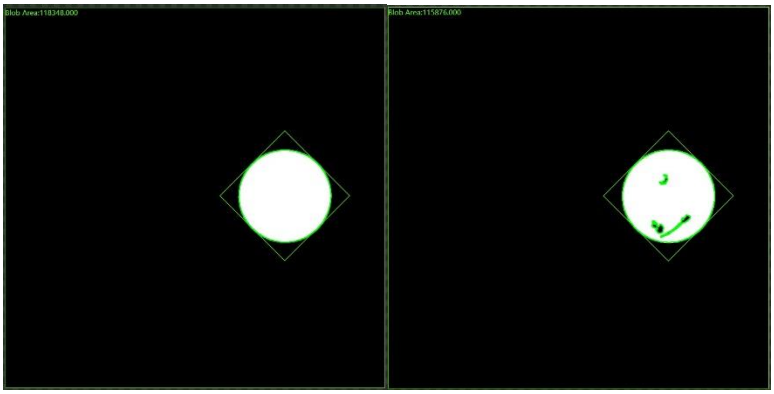

Figure 18: Trial 16- Wafer with Screw Dents (Predicted and Tested)

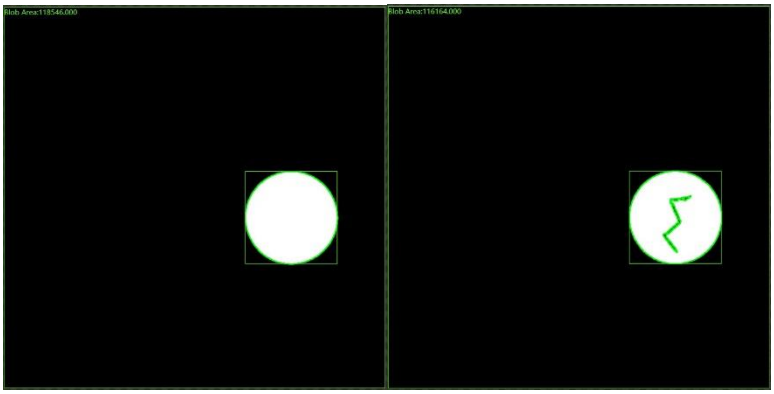

Figure 19: Trial 19- Wafer with Long Scratch (Predicted and Tested)

Figure 20: Trial 22- Wafer with Large Marker Blob (Predicted and Tested)

The results on plausible defects show the system is mostly capable of accurately identifying the location of these defects and output the correct response. The trials containing a wafer with box cuts (three thin cuts), wafers with bumps (0.5 mm and 1 mm), and a wafer with continuous marker dots (11 dots) correctly identified the defects each trial and the number of expected and actual defects were equal. In the trials containing wafers with screw dents (3 dents) and a long scratch (shaped like a lightning bolt) the system could correctly identify there was a defect however misidentified how many defects there were. In the trials containing misidentifications, a defect that was continuous would be broken into multiple segments causing additional defects to be reported. This is due to the roughly created defects containing shallow or thin portions that at different angles appear like the desired surface. Lastly, trials 22 to 24 were performed on a wafer with a large marker blob. The expectation for the system is to recognize this large defect however it does not. The reason for this is the area of the marker blob is greater than the 10,000 px upper bound specified in the previous section. Since testing was done on a wafer expected to be smooth, the upper bound limit could have been increased to have the marker blob detected.

5.2.3- System Lower Limitations

The surface analysis lower limitations of the system were tested to gain an understanding on the depth and diameter defects that could be inspected given the previously specified bounds. To test for this, two wafers were printed, one with dents containing varying depths and the other containing holes with varying diameters. The wafer containing dents had depths in millimeters of 1.41, 1.33, 1.27, 1.17, 1.01, 0.97, 0.90, 0.74, 0.60, 0.54, 0.44, 0.34, and 0.23. The wafer containing holes had diameters in millimeters of 2.6, 2.4, 2.25, 1.96, 1.80, 1.60, 1.42, 1.17, 0.93, and 0.66. The results from the inspections are provided below.

Trial	Item	System Result	Number of Detected Defects	Actual Number of Defects	Area of Predicted Item	Area of Examined Item
25	Varying Dent Depths	Defective	10	13	117366	104249
26	Varying Dent Depths	Defective	12	13	117119	99915
27	Varying Dent Depths	Defective	12	13	117401	101679
28	Varying Dent Widths	Defective	5	10	118079	115705
29	Varying Dent Widths	Defective	6	10	117839	115604

Table 11: System Lower Limitations

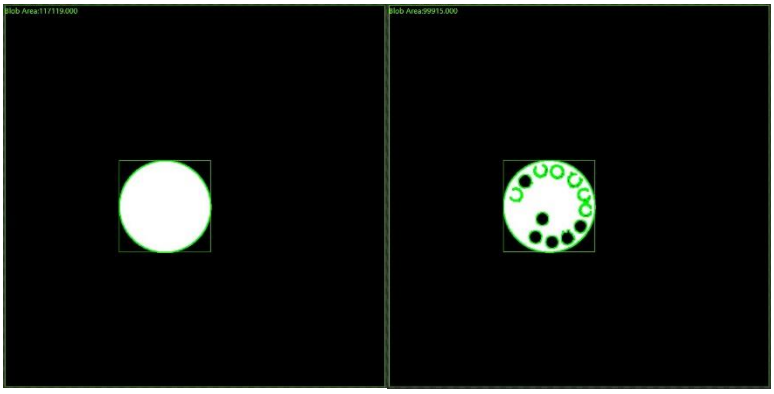

Figure 21: Trial 26- Wafer with Varying Dent Depths

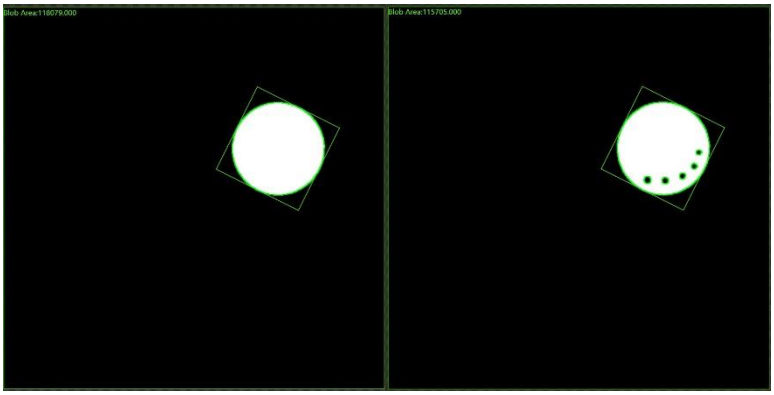

Figure 22: Trail 28- Wafer with Varying Hole Diameters

The results for the wafer with varying depths show the system could detect up to a depth of 0.54 mm. Not all trials resulted in the same number of defects which was expected since the defects were cleanly generated. The reason for this is likely due to how the lighting reflected off the shallow dents in certain locations on the inspection area. This issue can be overcome by improving the lighting source to better distribute light. Additionally, the defects on the upper half of Figure 21 are not complete circles. This is due to the kernel size in the sharpness filtering step brightening the pixels near it. Although reducing the kernel size could address this issue, maintaining edge sharpness was deemed more significant in the overall surface analysis. The results for the wafer with varying diameters show the system could detect up to the diameter of 1.60 mm. Again, the trial results did not have a consistent number of defects detected. The reason for this is partially needing to improve the lighting distribution as well as improving the resolution of the 3D printer used.

The surface analysis proposed in this QC system offers a technique for identifying any number of surface defects on an item. Some defects demonstrated in the previous sections were scratches, bumps, dents, and markings. These defects were selected because they are plausible in the manufacturing process. The overall performance of the QC system on surface inspection was acceptable. In all cases but one the system could identify the defects on the tested wafers. In the

large marker blob case, the system can be modified to account for it. Furthermore, the system's lower inspection limitations were demonstrated. The system could identify dents as shallow as 0.54 mm and holes as wide as 1.66 mm. Ultimately, the system could be used to automate inspection for many types of surface defects.

CHAPTER VI

INDUSTRY CASE STUDY

A QC case study using the proposed QC system was conducted on industrial parts. The industrial parts inspected were provided by Regal Beloit, a global manufacturer of electric motors, and are metal discs stacked to create rotors for their electric motors (Figure 23). Ensuring each metal disc is dimensionally correct or within a low error tolerance is essential to having the rotor mechanically operate as desired. Regal Beloit requires the metal discs have an outer diameter between 119.863 mm to 119.913 mm, an inner diameter between 34.011 mm to 34.036, and a slot length of 23.343 mm to 23.368 mm. A vision system is used by the company to perform dimensional inspections on sampled parts in the production line. The proposed QC system seeks to challenge the vision system used by Regal Beloit as well as offer surface inspections, capabilities of in-line inspections on all products, and remove the need for system training. In the following section the results achieved using the proposed QC system to inspect acceptable and defective discs will be described. Additionally, a section covering how the proposed QC system can be used in a production line with the provided industry parts is included.

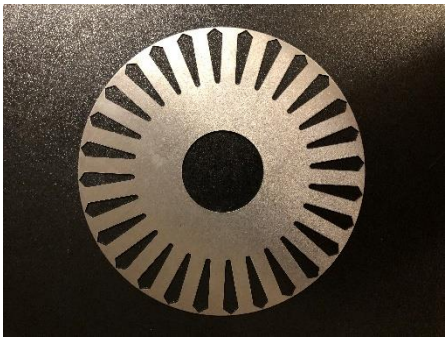

Figure 23: Metal Industry Disc

6.1- Industry Part Inspections

Adding defects for testing purposes to the few metal discs provided was not feasible. Therefore, to produce many discs containing unique defects, 3D printing offered the best alternative. Knowing the disc's desired dimensional specifications allowed for a computer aided design to be generated of it and facilitated in adding defects for system testing. The dimensional design alterations made to the disc were on outer diameter, inner diameter, and slot length. Once the designs (acceptable and defective) were completed, prints of them were made using white PLA material. The surface defects added were manually created with the design goal of plausibly occurring in a production line (e.g., scratches and dents).

6.1.1- Industry Parts Dimensional Analysis

The data used for dimensional analysis was collected from a base model disc fulfilling the desired dimensional specifications. 12 defect designs were created:

- Larger Outer Diameter (LOD) of 5%
- Larger Outer Diameter of 2%
- Larger Inner Diameter (LID) of 5%
- Larger Inner Diameter of 2%

- Longer Slots (LS) of 1 mm
- Longer Slots of 0.5 mm
- Shorter Slots (SS) of 1 mm
- Shorter Slots of 0.5 mm
- Smaller Outer Diameter (SOD) of 5%
- Smaller Outer Diameter of 2%
- Smaller Inner Diameter (SID) of 5%
- Smaller Inner Diameter of 2%

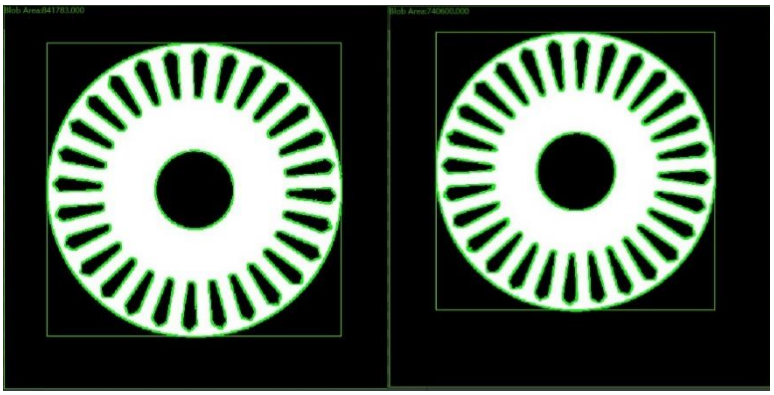

Figure 24: (left) Larger Outer Diameter 5%, (right) Smaller Inner Diameter 5%

The results from the dimensional testing is provided in Appendix A. A likeness score of 1 indicates an item is perfectly equal in perimeter, area, circularity, and rectangularity to a base item. All trials used the same light intensity, product type, and image resolution. The table columns are organized by trial, the base item and parameter values generated in that trial, the tested item and parameter values generated in that trial, and a likeness score. Each defective item had five trials performed for it. A statistical summary is provided in Table 11 on the dimensional analysis results. Measurements in millimeters were taken of the 3D printed discs using a digital caliper and are provided in Table 12.

Test Design	Average Likeness Score	Standard Deviation Likeness Score	Max Likeness Score	Min Likeness Score
Original	0.9964	0.000548	0.997	0.996
LOD 5%	0.9264	0.002302	0.929	0.924
LOD 2%	0.9662	0.001924	0.968	0.963
SOD 5%	0.9198	0.002168	0.922	0.917
SOD 2%	0.963	0.001000	0.964	0.962
LS 1 mm	0.995	0.001000	0.996	0.994
LS 0.5 mm	0.9964	0.003131	0.999	0.991
SS 0.5 mm	0.996	0.001581	0.998	0.994
SS 1 mm	0.995	0.002000	0.997	0.993
SID 2%	0.9944	0.000894	0.995	0.993
SID 5%	0.9916	0.001140	0.993	0.99
LID 5%	0.9866	0.002510	0.99	0.983
LID 2%	0.9908	0.001483	0.993	0.989

Table 12: Industry Disc Dimensional Analysis Statistics

Part	Outer Diameter (mm)	Inner Diameter (mm)	Slot Length (mm)
Original	119.95	33.94	22.60
SS 1mm	119.97	33.70	22.05
SS 0.5mm	119.82	33.72	22.21

LS 0.5mm	119.76	33.77	22.82
LS 1mm	119.81	33.82	23.19
LID 2%	120.07	34.47	21.72
LID 5%	119.83	35.55	21.54
LOD 2%	122.18	33.75	21.72
LOD 5%	125.69	33.72	21.61
SID 5%	119.95	32.05	22.61
SID 2%	119.91	33.21	22.72
SOD 2%	117.65	33.87	23.14
SOD 5%	113.65	33.96	22.63

Table 13: Measurements of 3D Printed Discs

The statistical results from Table 11 show the proposed MV system can detect millimeter level defects on products. The original-to-original trials (base compared to acceptable test) had a high average likeness score of 0.9964 and a standard deviation of 0.000548. The reason for the likeness score not being perfect is due to noise during image acquisition and minor errors occurring in producing the discs.

The results from the larger and smaller outer diameter trials had the lowest likeness scores, which is expected because changing the outer diameter has a significant impact on perimeter and area for the discs. The smaller diameter of 5% and larger diameter of 5% have a nearly equal likeness score to each other as well as the smaller diameter of 2% and larger diameter of 2% to each other. This is due to the dimensional analysis algorithm taking the absolute difference between the base and test items. The likeness scores for outer diameter prove the proposed MV system can accurately detect defective discs with an outer diameter of 2 mm

less than or greater than the desired specification (Table 12 provides physical distance measurements).

The results for the longer and shorter slots on the discs had likeness scores much closer on average to 1. It worth noting that although the slots were designed to be longer or shorter by a millimeter or half a millimeter, the printed slots defects were measured to be about half that (Table 12). The reason for the high likeness scores is due to the slot size changes only marginally affecting the disc area, circularity, and rectangularity. Future work will attempt to improve identifying these finer differences within an item by enhancing the image acquisition resolution and modifying the algorithm to better consider these defects.

The results for the larger and shorter inner diameters were higher than desired and contained greater variability than the other defect types. Since only the outer perimeter of an item is measured, this significant parameter was not considered by the algorithm for the changed inner diameter. Future work will attempt to improve this lacking detection feature.

6.1.2- Industry Parts Surface Analysis

As mentioned in chapter 5, the surface analysis performed by the proposed QC system does not compare test items to a base model. Three surface defects were added separately to industry discs: 1) dents created using a screwdriver, 2) scratches created using a box cutter, and 3) black marks created using a marker. The results from the surface inspection on the industry discs is shown in Table 13. The image outputs from the blob analysis on the tested items are shown in Figures 25-27.

Trial	Item	Result	Number of Detected Defects	Expected Number of Defects	Area of Predicted Base	Area of Tested Item
1	Disc Dents	Defective	4	4	694434	691601
2	Disc Dents	Defective	4	4	694462	691847
3	Disc Scratches	Defective	2	2	793613	791160
4	Disc Scratches	Defective	2	2	793867	791559
5	Disc Marks	Defective	4	4	695684	693834
6	Disc Marks	Defective	4	4	695295	693431

Table 14: Industry Discs Surface Results

Figure 25: Industry Disc Surface Dents

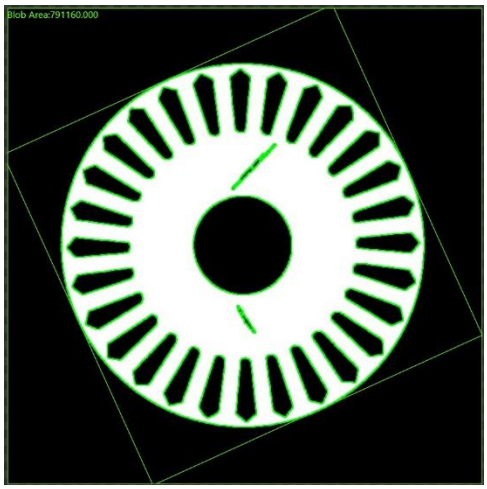

Figure 26: Industry Disc Surface Scratches

Figure 27: Industry Disc Surface Marks

The results in Table 13 show that the QC system could correctly identify the defects on the discs at a 100% accuracy. Ultimately, the surface analysis proposed provides an additional inspection technique to ensure that QC is maintained in the production of these industrial discs. Adding surface analysis to the vision inspection already performed at Regal Beloit could prevent discs containing rust, holes, or bumps from being used in their electric motors.

6.2- A Simulated Inspection Line

The practicality of the proposed QC system is demonstrated in this section through use in a possible production line inspection scenario. The scenario involves using the automated

inspection system to identify acceptable and defective industry discs considered in the previous section, and then based on the system output correctly transferring the discs to a location. The equipment used in this scenario is the QC system, a Dobot desktop robotic arm and two conveyor belts (Figure 28). The robotic arm is placed in front of the QC system rig and a conveyor belt is place on each side of the robotic arm. One conveyor belt moves discs needed for inspection within reach of the robotic arm. The robotic arm then uses its suction cup end-effector to lift and place the disc in the inspection area. The robotic arm moves out-of-view from the inspection area for the QC system to complete its tasks. Next, the robotic arm lifts the disc and places it on the other conveyor belt. Once on the conveyor belt, the disc will move one way if deemed acceptable by the system or move the other way if defective. The robotic arm was taught to move to specified points which is sufficient for the purpose of demonstrating the use of the QC system.

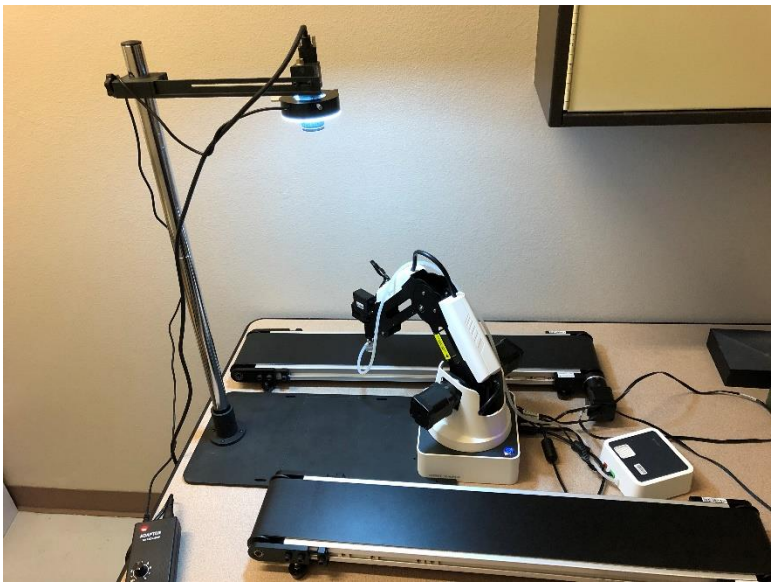

Figure 28: Production Line Inspection Scenario

Two tests were performed on the industry discs using the inspection scenario. In each test four discs were used, the base disc and three defective discs. The inspection begins with the base item since the dimensions of it are needed to judge test discs. The base item is automatically

moved by the second conveyor belt to the acceptable item's direction. The other three discs containing either a dimensional defect, surface defect, or both are judged. If the item contains at least one defect, it is entirely labelled defective. Finally, to prove the system not only judges defective items correctly, the base item used in each test is put back on the conveyor belt for inspection. The results from both tests are shown in Table 14. A likeness score of 0.99 or greater is the accepted range for dimensional analysis.

Test	**Defect**	**Dim Analysis**	**Likeness Score**	**Surface Analysis**
1	1 mm SS and Marks	Defective	0.986	Defective
1	Original Dim and Bumps	Acceptable	0.99	Defective
1	Original Dim and Dents	Acceptable	0.992	Defective
1	Base	Acceptable	0.997	Acceptable
2	SOD 2%	Defective	0.966	Acceptable
2	SID 2%	Defective	0.988	Acceptable
2	LOD 5% and Cuts	Defective	0.924	Defective
2	Base	Acceptable	0.998	Acceptable

Table 15: Production Line Inspection Test Results

The results in Table 14 show acceptable or defective (depending on whether it passed or failed a test) for each analysis on a test disc. All test discs correctly had their expected defects identified by the system. The disc containing slots 1 mm short and marks on its surface and the disc with an outer diameter larger by 5% and box cuts on its surface had both defects correctly identified. The remaining defective discs each had their respective defects correctly identified while otherwise being acceptable. The two base items inspected had both analyses deemed acceptable with high likeness scores.

Overall, the presented case study tests the capabilities of the proposed QC system to be applied on an industry case study. The dimensional analysis performed on the industry discs shows the QC system could identify extremely fine differences between discs and is a promising industrial alternative for this form of inspection. The surface analyses performed could identify all surface defects at a 100% accuracy, except for the large marker blob due to its size. Adjustments to the system's parameters can be made to extend the range of identifiable defects. Lastly, the system was integrated in a production line scenario to demonstrate its automated capabilities. In each trial for each test the correct outputs were given regarding dimensional and surface analysis. The production line scenario also demonstrates that the small sized QC system can be added in existing production lines. This minimal volume system would replace the larger inspection machines currently used that are disconnected from the production line and requiring manual handling for inspection.

CHAPTER VII

CONCLUSION

7.1- Conclusion

QC will forever be present in a manufacturing world containing even the slightest possibility of error. Due to this ever-present problem, major advancements in QC have been made in industry to reduce cost and time needed for product inspections. QC systems using MV are presently a state-of-the-art technology allowing both cost and time to be driven down while operating accurately and precisely. The QC system proposed in this thesis offers a product inspection solution that meets the cost and time demands as well as offers improved adaptability, automation, and robustness in inspections. Recent literature on QC systems using MV offers a variety of dimensional and surface analysis solutions for varying applications. In this literature, most of the work uses ML to develop advanced recognition capabilities for a single item or small set. The proposed QC system builds on the literature by simultaneously performing dimensional and surface inspections without the need for model training. The results achieved in Chapter 4 on dimensional analysis demonstrated the system could identify diverse shapes that were simple or complex. Furthermore, the cube testing in Chapter 4.4 demonstrated the system could accurately identify millimeter differences. The results in Chapter 5 on surface analysis proved the system could determine whether surface defects were present and locate them. Although minor assumptions are made on the items and their possible defects, it was discussed that altering the

system's setting could provide greater flexibility in item designs. All but one of the surface items inspected (large marker blob) had their defects located and outputted. Finally, the case study on the industry discs provided by Regal Beloit were converted to 3D printed plastic and altered to test the system's performance. The proposed QC system offers solutions to the existing challenges in industrial QC, such as those faced by Regal Beloit, through the following benefits: dimensional analysis, surface analysis, high repeatability, automated inspection with no system training needed other than providing a base item, and in-line vision inspection. Ultimately, the proposed QC system provides an automated visual inspection using robust techniques for production lines.

7.2- Future Work

The proposed QC system demonstrated accurate and precise visual inspection capabilities. However, improvements to the MV can be made to continue facilitating this form of QC and having its results more reliable. Allowing the system to operate properly in environments containing light other than from the system's light source would further its practicality. By allowing the system to handle environments with varying light, opportunities arise for outdoor use. Additionally, improving the scale the system can detect at would allow for a greater range of inspectable items. In the case study presented, a very fine level of detail was required for inspection which the system's results could have been improved by including. Allowing the QC system to inspect at the microscale range would allow for medical device equipment to be inspected. Next, the QC system only inspects two-dimensionally but if expanded to three-dimensions could provide a more comprehensive analysis of an item. Items that do not contain equal cross-sectional areas could be inspected and data such as item volume

could be collected. Improvements to the proposed algorithm should be made to better account for dimensional interior differences and to allow for a greater range of surface designs to be inspected. Ultimately, ML was commonly used in the literature survey conducted in Chapter 2. Adopting ML to the proposed QC system could allow for more informed decisions to the dimensional and surface analyses. For dimensional analysis, ML could provide output information on what about products is dimensionally defective. For surface analysis, ML could allow for categorization of defects, such as whether a defect is a dent or scratch. Convolutional neural networks (CNN) are a popular ML technique that applies the advantages of neural networks to image processing. Using CNN is as a ML technique to improve the performance of the proposed QC system will be explored in the future.

REFERENCES

1. Russell, J.P. The ASQ Auditing Handbook, Fourth Edition, 2012, asq.org/quality-press/display-item?item=H1435.
2. Eiríksson, Eyþór Rúnar. "Computer Vision for Additive Manufacturing." (2018).
3. Dai, Yiquan, and Kunpeng Zhu. "A machine vision system for micro-milling tool condition monitoring." Precision engineering 52 (2018): 183-191.
4. Bolton, Brian E. “Eight Data Acquisition Best Practices.” Control Engineering, 26 Nov. 2019, www.controleng.com/articles/eight-data-acquisition-best-practices/.
5. Kujawińska, Agnieszka, and Katarzyna Vogt. "Human factors in visual quality control." Management and Production Engineering Review 6 (2015).
6. Jakobsson, Olafur P. "Database interface for digital calipers." Computer methods and programs in biomedicine 28.1 (1989): 51-55.
7. Kackar, Raghu N. "Off-line quality control, parameter design, and the Taguchi method." journal of Quality Technology 17.4 (1985): 176-188.
8. Gamer, Thomas, et al. "The Autonomous Industrial Plant-Future of Process Engineering, Operations and Maintenance." IFAC-PapersOnLine 52.1 (2019): 454-460.
9. de Sousa Junior, Wilson Trigueiro, et al. "Shop floor simulation optimization using machine learning to improve parallel metaheuristics." Expert Systems with Applications 150 (2020): 113272.

10. Hewitt, Phil. “Inspection in the Age of Smart Manufacturing.” Technology | Manufacturing Global, 23 Oct. 2018, www.manufacturingglobal.com/technology/inspection-age-smart-manufacturing.
11. Péter, Gábor, Bálint Kiss, and Viktor Tihanyi. "Vision and odometry based autonomous vehicle lane changing." ICT Express 5.4 (2019): 219-226.
12. García, Cristian González, et al. "Midgar: Detection of people through computer vision in the Internet of Things scenarios to improve the security in Smart Cities, Smart Towns, and Smart Homes." Future Generation Computer Systems 76 (2017): 301-313.
13. Singh, Arun Kumar, et al. "Vision based rail track extraction and monitoring through drone imagery." ICT Express 5.4 (2019): 250-255.
14. Hosseinpour, Soleiman, Ali Hakimi Ilkhchi, and Mortaza Aghbashlo. "An intelligent machine vision-based smartphone app for beef quality evaluation." Journal of Food Engineering 248 (2019): 9-22.
15. Alonso, Victor, et al. "Industry 4.0 implications in machine vision metrology: an overview." Procedia Manufacturing 41 (2019): 359-366.
16. Paul, Nicholas, and ChanJin Chung. "Application of HDR algorithms to solve direct sunlight problems when autonomous vehicles using machine vision systems are driving into sun." Computers in Industry 98 (2018): 192-196.
17. Shin, Jaemyung, et al. "Effect of directional augmentation using supervised machine learning technologies: A case study of strawberry powdery mildew detection." Biosystems Engineering 194 (2020): 49-60.
18. Sylla, Cheickna. "Experimental investigation of human and machine-vision arrangements in inspection tasks." Control Engineering Practice 10.3 (2002): 347-361.

19. Pacella, Massimo, Antonio Grieco, and Marzia Blaco. "Machine vision based quality control of free-form profiles in automatic cutting processes." Computers & Industrial Engineering 109 (2017): 221-232.
20. Chethan, Y. D., H. V. Ravindra, and Y. T. Krishnegowda. "Optimization of machining parameters in turning Nimonic-75 using machine vision and acoustic emission signals by Taguchi technique." Measurement 144 (2019): 144-154.
21. Wang, Chao, et al. "Research on the classification algorithm and operation parameters optimization of the system for separating non-ferrous metals from end-of-life vehicles based on machine vision." Waste Management 100 (2019): 10-17.
22. Su, Qinghua, et al. "Potato quality grading based on machine vision and 3D shape analysis." Computers and electronics in agriculture 152 (2018): 261-268.
23. Williams, Henry AM, et al. "Robotic kiwifruit harvesting using machine vision, convolutional neural networks, and robotic arms." biosystems engineering 181 (2019): 140-156.
24. Zhou, Chao, et al. "Evaluation of fish feeding intensity in aquaculture using a convolutional neural network and machine vision." Aquaculture 507 (2019): 457-465.
25. Azarmdel, Hossein, et al. "Developing an orientation and cutting point determination algorithm for a trout fish processing system using machine vision." Computers and Electronics in Agriculture 162 (2019): 613-629.
26. Wang, S. Y., et al. "A computer vision based machine learning approach for fatigue crack initiation sites recognition." Computational Materials Science 171 (2020): 109259.

27. Lies, Benjamin T., et al. "Machine vision assisted micro-filament detection for real-time monitoring of electrohydrodynamic inkjet printing." Procedia Manufacturing 26 (2018): 29-39.
28. Martinez, Pablo, Rafiq Ahmad, and Mohamed Al-Hussein. "A vision-based system for pre-inspection of steel frame manufacturing." Automation in Construction 97 (2019): 151-163.
29. Moru, Desmond K., and Diego Borro. "A machine vision algorithm for quality control inspection of gears." The International Journal of Advanced Manufacturing Technology 106.1-2 (2020): 105-123.
30. Devi, T. Gayathri, P. Neelamegam, and S. Sudha. "Machine vision based quality analysis of rice grains." 2017 IEEE International Conference on Power, Control, Signals and Instrumentation Engineering (ICPCSI). IEEE, 2017.
31. Chen, Shumian, et al. "Colored rice quality inspection system using machine vision." Journal of cereal science 88 (2019): 87-95.
32. Xie, Weijun, Fenghe Wang, and Deyong Yang. "Research on Carrot Grading Based on Machine Vision Feature Parameters." IFAC-PapersOnLine 52.30 (2019): 30-35.
33. Huang, Bin, et al. "Research and implementation of machine vision technologies for empty bottle inspection systems." Engineering science and technology, an international journal 21.1 (2018): 159-169.
34. Kazemian, Ali, et al. "Computer vision for real-time extrusion quality monitoring and control in robotic construction." Automation in Construction 101 (2019): 92-98.
35. Iglesias, Carla, Javier Martínez, and Javier Taboada. "Automated vision system for quality inspection of slate slabs." Computers in Industry 99 (2018): 119-129.

36. Lee, Yi-Cheng, and Syh-Shiuh Yeh. "Using Machine Vision to Develop an On-Machine Thread Measurement System for Computer Numerical Control Lathe Machines." Lecture Notes in Engineering and Computer Science: Proceedings of The International MultiConference of Engineers and Computer Scientists. 2019.
37. Joshi, Ketaki, and Bhushan Patil. "Prediction of Surface Roughness by Machine Vision using Principal Components based Regression Analysis." Procedia Computer Science 167 (2020): 382-391.
38. Wang, Jinjiang, Peilun Fu, and Robert X. Gao. "Machine vision intelligence for product defect inspection based on deep learning and Hough transform." Journal of Manufacturing Systems 51 (2019): 52-60.
39. Sudhagar, S., M. Sakthivel, and P. Ganeshkumar. "Monitoring of friction stir welding based on vision system coupled with Machine learning algorithm." Measurement 144 (2019): 135-143.
40. Kumar, S. Dhakshina, et al. "A Microcontroller based Machine Vision Approach for Tomato Grading and Sorting using SVM Classifier." Microprocessors and Microsystems (2020): 103090.
41. Smith, Lyndon Neal, et al. "Innovative 3D and 2D machine vision methods for analysis of plants and crops in the field." Computers in industry 97 (2018): 122-131.
42. Woodham, Robert J. "Photometric method for determining surface orientation from multiple images." Optical engineering 19.1 (1980): 191139.
43. Asaei, Habil, Abdolabbas Jafari, and Mohammad Loghavi. "Site-specific orchard sprayer equipped with machine vision for chemical usage management." Computers and Electronics in Agriculture 162 (2019): 431-439.

44. Zhuang, J. J., et al. "Detection of orchard citrus fruits using a monocular machine vision-based method for automatic fruit picking applications." Computers and Electronics in Agriculture 152 (2018): 64-73.1

45. Kumar, Varun, and CP Sudheesh Kumar. "Investigation of the influence of coloured illumination on surface texture features: A Machine vision approach." Measurement 152 (2020): 107297.

APPENDIX A

APPENDIX A

INDUSTRY DISC DIMENSIONAL ANALYSIS

Trial	Base Design	Base Area	Base Perimeter	Base Circularity	Base Rectangularity	Test Design	Test Area	Test Perimeter	Base Circularity	Base Rectangularity	Likeness Score
1	Original	737843.000	4003.989	0.680	0.541	LOD 5%	839093.000	4174.617	0.700	0.559	0.928
2	Original	737303.000	3991.421	0.681	0.540	LOD 5%	839423.000	4200.558	0.700	0.559	0.924
3	Original	735107.000	3931.556	0.682	0.539	LOD 5%	836918.000	4134.634	0.688	0.558	0.927
4	Original	735906.000	3951.941	0.683	0.539	LOD 5%	837684.000	4156.131	0.702	0.559	0.924
5	Original	740290.000	4068.516	0.683	0.542	LOD 5%	841783.000	4225.854	0.703	0.561	0.929
6	Original	737655.000	4001.078	0.684	0.540	LOD 2%	781252.000	4070.274	0.697	0.551	0.967
7	Original	737372.000	3981.279	0.679	0.541	LOD 2%	780868.000	4079.320	0.689	0.550	0.966
8	Original	738797.000	4006.308	0.665	0.541	LOD 2%	780773.000	4051.379	0.692	0.550	0.968
9	Original	738442.000	4002.592	0.674	0.542	LOD 2%	781066.000	4077.546	0.689	0.551	0.967
10	Original	740382.000	4018.090	0.682	0.542	LOD 2%	783214.000	4153.712	0.691	0.552	0.963

11	Original	738820.000	3996.492	0.682	0.541	LID 5%	729664.000	4035.930	0.665	0.534	0.987
12	Original	738746.000	4023.404	0.683	0.541	LID 5%	729251.000	4041.546	0.659	0.534	0.987
13	Original	728070.000	4011.119	0.658	0.533	LID 5%	738083.000	4019.847	0.683	0.541	0.986
14	Original	728325.000	4044.215	0.671	0.533	LID 5%	737712.000	4011.220	0.675	0.540	0.990
15	Original	740878.000	4037.930	0.683	0.542	LID 5%	730454.000	4092.742	0.659	0.535	0.983
16	Original	736619.000	3970.651	0.679	0.540	LID 2%	729131.000	3981.296	0.672	0.534	0.993
17	Original	737004.000	3996.333	0.680	0.540	LID 2%	729367.000	3983.740	0.669	0.534	0.991
18	Original	738040.000	4022.291	0.681	0.541	LID 2%	729661.000	3986.065	0.674	0.535	0.990
19	Original	738248.000	3996.065	0.678	0.540	LID 2%	729625.000	3960.367	0.676	0.535	0.991
20	Original	740478.000	4030.232	0.684	0.542	LID 2%	730643.000	4048.700	0.673	0.535	0.989
21	Original	737751.000	4005.504	0.682	0.540	LS 1 mm	732276.000	3999.604	0.676	0.537	0.995
22	Original	738817.000	4023.587	0.684	0.541	LS 1 mm	734237.000	3995.948	0.681	0.538	0.994
23	Original	737778.000	4000.249	0.680	0.541	LS 1 mm	733449.000	4012.090	0.669	0.538	0.994

24	Original	737604.000	3995.078	0.680	0.540	LS 1 mm	734078.000	3984.107	0.682	0.538	0.996
25	Original	740412.000	4036.274	0.681	0.542	LS 1 mm	736562.000	4044.960	0.676	0.540	0.996
26	Original	739577.000	4030.717	0.683	0.542	LS 0.5 mm	738008.000	4037.830	0.682	0.540	0.998
27	Original	739393.000	3997.504	0.684	0.541	LS 0.5 mm	738184.000	4005.161	0.683	0.541	0.999
28	Original	738156.000	3989.823	0.684	0.541	LS 0.5 mm	737328.000	4009.320	0.680	0.540	0.997
29	Original	737814.000	3975.823	0.683	0.541	LS 0.5 mm	737554.000	4001.705	0.683	0.540	0.997
30	Original	740253.000	4054.315	0.680	0.542	LS 0.5 mm	738770.000	4095.913	0.659	0.540	0.991
31	Original	739958.000	4074.298	0.685	0.542	SS 0.5 mm	741318.000	4131.050	0.684	0.543	0.994
32	Original	741280.000	4088.055	0.681	0.542	SS 0.5 mm	742224.000	4100.641	0.684	0.543	0.998

33	Original	741390.000	4095.771	0.680	0.543	SS 0.5 mm	743274.000	4128.967	0.684	0.544	0.995
34	Original	741405.000	4091.529	0.677	0.542	SS 0.5 mm	744198.000	4095.854	0.678	0.545	0.997
35	Original	740614.000	4036.960	0.682	0.543	SS 0.5 mm	742567.000	4064.232	0.682	0.544	0.996
36	Original	741390.000	4084.198	0.677	0.543	SS 1 mm	743958.000	4086.499	0.682	0.544	0.997
37	Original	742820.000	4085.938	0.685	0.543	SS 1 mm	744709.000	4057.286	0.681	0.545	0.995
38	Original	742658.000	4103.209	0.674	0.543	SS 1 mm	744826.000	4069.712	0.686	0.545	0.993
39	Original	742333.000	4065.411	0.677	0.543	SS 1 mm	744581.000	4065.813	0.682	0.545	0.997
40	Original	739987.000	4015.930	0.678	0.542	SS 1 mm	743044.000	4041.161	0.664	0.543	0.993
41	Original	742374.000	4073.813	0.672	0.543	SOD 5%	638216.000	3877.504	0.650	0.518	0.922
42	Original	742299.000	4058.274	0.680	0.542	SOD 5%	639293.000	3877.823	0.644	0.517	0.921
43	Original	742009.000	4071.185	0.682	0.542	SOD 5%	638992.000	3855.622	0.647	0.518	0.918
44	Original	741392.000	4024.090	0.679	0.543	SOD 5%	637398.000	3875.338	0.637	0.516	0.921

45	Original	741945.000	4066.132	0.683	0.542	SOD 5%	637408.000	3859.237	0.645	0.516	0.917
46	Original	736509.000	3956.267	0.681	0.540	SOD 2%	688524.000	3880.928	0.660	0.524	0.962
47	Original	738480.000	3977.095	0.681	0.541	SOD 2%	690302.000	3921.136	0.661	0.525	0.963
48	Original	738660.000	3984.634	0.683	0.541	SOD 2%	690552.000	3919.722	0.662	0.525	0.962
49	Original	740789.000	4016.533	0.678	0.542	SOD 2%	691974.000	3952.835	0.664	0.526	0.964
50	Original	739835.000	4032.031	0.682	0.542	SOD 2%	692112.000	3974.877	0.661	0.526	0.964
51	Original	740477.000	4044.031	0.681	0.542	SID 2%	746435.000	4064.901	0.683	0.545	0.994
52	Original	740465.000	4023.906	0.681	0.542	SID 2%	745810.000	4039.060	0.684	0.545	0.995
53	Original	740418.000	4054.073	0.680	0.542	SID 2%	746101.000	4083.587	0.683	0.545	0.993
54	Original	740209.000	4031.847	0.681	0.542	SID 2%	745712.000	4041.019	0.685	0.545	0.995
55	Original	740315.000	4039.345	0.682	0.541	SID 2%	745812.000	4026.676	0.682	0.545	0.995
56	Original	739966.000	4028.776	0.680	0.542	SID 5%	748838.000	4009.664	0.687	0.548	0.991
57	Original	741271.000	4033.889	0.684	0.542	SID 5%	748247.000	4017.102	0.691	0.548	0.992

58	Original	740920.000	4031.019	0.683	0.543	SID 5%	748016.000	4050.776	0.687	0.548	0.993
59	Original	740218.000	4031.705	0.681	0.542	SID 5%	748467.000	4059.445	0.691	0.548	0.990
60	Original	740600.000	4033.320	0.682	0.542	SID 5%	748903.000	4027.504	0.693	0.548	0.992

BIOGRAPHICAL SKETCH

Mark Anthony Reyna earned a B.A. Economics degree from the University of Texas at Austin from 2015 to 2019. While at the University of Texas at Austin, Mark also earned the Elements of Computing Certificate for his coursework in computer science. Mark followed his bachelor's degree with a Master's in Electrical Engineering earned in May 2021 at the University of Texas Rio Grande Valley. His specialization is in automated quality control using machine vision systems. After graduating, Mark joined Boston Scientific, a global leader in medical device equipment, as a Process Engineer in Maple Grove, Minnesota. Mark Reyna may be contacted via email at markreyna96@gmail.com.